Shaker Potassium Channel Gating III: Evaluation of Kinetic Models for Activation

WILLIAM N. ZAGOTTA, TOSHINORI HOSHI, and RICHARD W. ALDRICH

From the Department of Molecular and Cellular Physiology, Howard Hughes Medical Institute, Stanford University School of Medicine, Stanford, California 94305

ABSTRACT Predictions of different classes of gating models involving identical conformational changes in each of four subunits were compared to the gating behavior of *Shaker* potassium channels without N-type inactivation. Each model was tested to see if it could simulate the voltage dependence of the steady state open probability, and the kinetics of the single-channel currents, macroscopic ionic currents and macroscopic gating currents using a single set of parameters. Activation schemes based upon four identical single-step activation processes were found to be incompatible with the experimental results, as were those involving a concerted, opening transition. A model where the opening of the channel requires two conformational changes in each of the four subunits can adequately account for the steady state and kinetic behavior of the channel. In this model, the gating in each subunit is independent except for a stabilization of the open state when all four subunits are activated, and an unstable closed conformation that the channel enters after opening. A small amount of negative cooperativity between the subunits must be added to account quantitatively for the dependence of the activation time course on holding voltage.

INTRODUCTION

In the preceding two papers (Hoshi, Zagotta, and Aldrich, 1994; Zagotta, Hoshi, Dittman, and Aldrich, 1994) we have identified a number of general properties of the activation gating mechanism in *Shaker* potassium channels. These include the following: (*a*) The activation conformational changes are associated with the movement of charge equivalent to 12 to 16 electronic charges through the membrane electric field. (*b*) Opening of the channel from hyperpolarized voltages requires more

Address correspondence to Richard W. Aldrich, Department of Molecular and Cellular Physiology, Stanford University School of Medicine, Stanford, CA 94305-5426.

Dr. Zagotta's present address is Department of Physiology and Biophysics, SJ-40, University of Washington, Seattle, WA 98195.

Dr. Hoshi's present address is Department of Physiology and Biophysics, University of Iowa, Iowa City, IA 52242-1109.

J. GEN. PHYSIOL. © The Rockefeller University Press · 0022-1295/94/02/0321/42 $2.00
Volume 103 February 1994 321–362

than five sequential conformational changes. (*c*) The total charge movement is spread out among many or all of these conformational changes and resides more in the reverse transitions than in the forward transitions. (*d*) Once open, the channel can enter closed states that are not directly in the activation pathway. (*e*) The first closing transition is slower than expected for a model involving a number of independent and identical transitions.

In this paper we extend our analysis of the kinetics of ShBΔ6-46 channels to consider a number of specific kinetic schemes to account for the phenomena discussed in the previous two papers (Hoshi et al., 1994; Zagotta et al., 1994). The development of a quantitative model to describe the activation gating mechanism is important for several reasons. It provides a quantitative test of whether the proposed mechanism can simultaneously account for all of the observations. In addition, a model provides a framework for the interpretation of the results of structural alterations that alter the channel's gating behavior. This framework provides insights into the molecular mechanisms of the conformational changes involved in gating.

Because it is likely that *Shaker* channels exist as homotetramers in *Xenopus* oocytes (MacKinnon, 1991), we have restricted our analysis to kinetic schemes that can be interpreted in terms of four identical subunits. This restriction on the types of models considered was important for several reasons. It greatly reduced the number of potential kinetic schemes to a more manageable number. Furthermore, it makes use of the knowledge of the subunit composition that provides valuable clues about the physical mechanism underlying the kinetic behavior. If a model is developed with the subunit composition in mind, its kinetic transitions are also more easily interpreted in terms of physical conformational changes in the channel protein. In addition, the model can provide a possible physical explanation for the effects of mutations in the protein structure on the kinetic behavior.

The models considered in this paper all contain identical conformational changes, or sets of conformational changes, occurring in each of four subunits. Identical conformational changes, in this context, means that the same physical rearrangements are occurring within each subunit, so the charge movement and associated voltage dependence of the transitions are identical. It does not mean that the transitions are independent, or that they are occurring with the same rate. Models are considered with nonindependent transitions between subunits, such as cooperative transitions, concerted conformational changes, and slowed first closing transitions. The conformational states and conformational transitions are modeled as time-homogeneous Markov processes with rate constants for the voltage-dependent transitions that are exponentially dependent on voltage. These commonly used assumptions are reasonable for the modeling of gating conformational changes (McManus and Magleby, 1989; McManus, Spivak, Blatz, Weiss, and Magleby, 1989; Stevens, 1978).

MATERIALS AND METHODS

Experiments, data analysis and simulation were carried out as described in the two proceeding papers (Hoshi et al., 1994; Zagotta et al., 1994). The values of the parameters in the models in Fig. 7 and 17 were first estimated from the chi-squared fits to the data presented in the two preceding papers and this paper. These values were then adjusted to optimize the overall fits.

RESULTS

Several classes of kinetic models are shown in Fig. 1. In each case where it is practical, the model is shown in an extended format showing all of the kinetic states and in an abbreviated format that emphasizes the conformational transitions occurring within each subunit. These models show only the transitions in the activation pathway. In general, the channel may also undergo transitions to other states not directly in the activation pathway, as discussed in the first paper (Hoshi et al., 1994). For class A

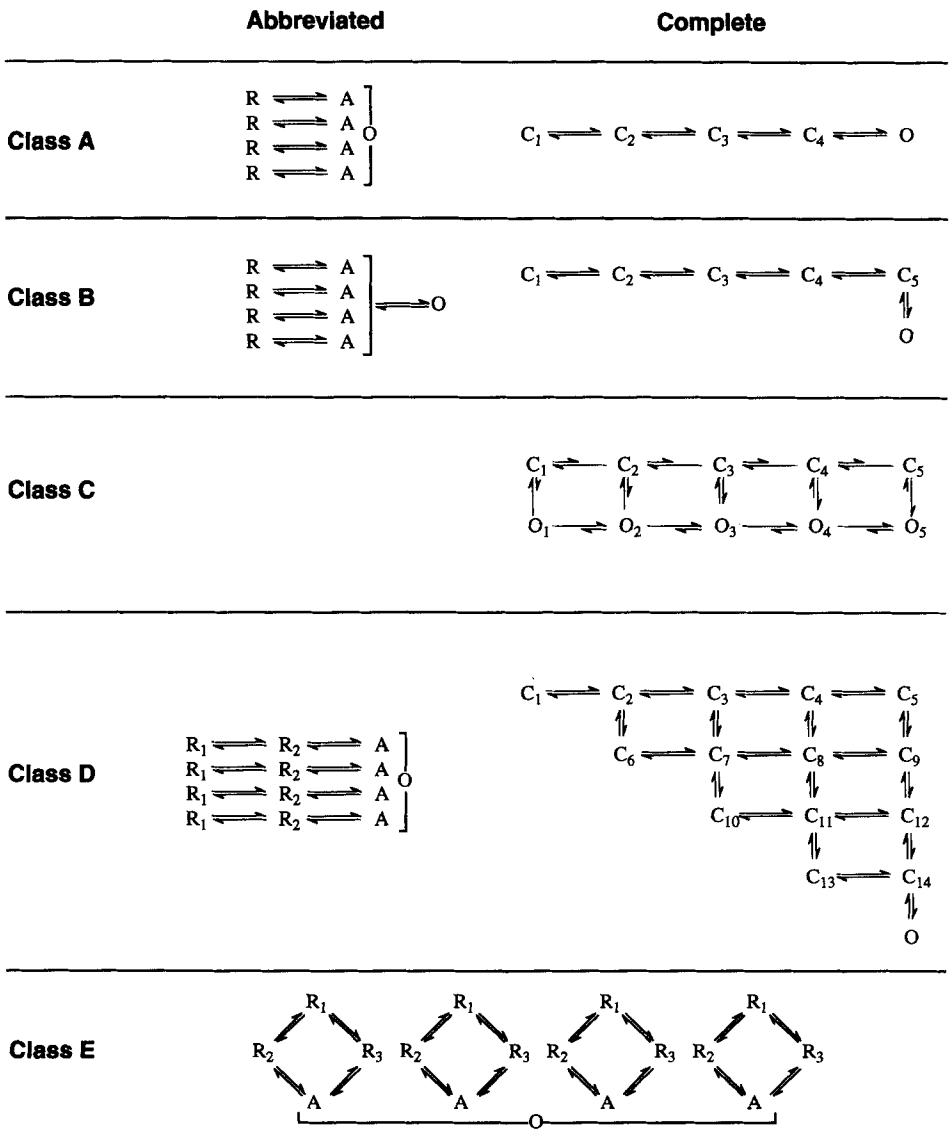

FIGURE 1. Five classes of the models considered in the paper. See the main text for details.

models, the opening of the channel requires only a single conformational change in each subunit. This class is typified by the scheme of Hodgkin and Huxley (1952) involving four independent and identical transitions to explain the activation gating of a voltage-dependent potassium channel from squid axons. In general, however, the transitions would not have to be independent (Armstrong, 1981; Gilly and Armstrong, 1982; Hill and Chen, 1971*a,b;* Vandenberg and Bezanilla, 1991). Class B postulates that, after undergoing a single conformation change in each subunit, the channel must undergo a final, concerted conformational change to open. The voltage dependence and kinetics of the concerted conformational change would, in general, be different from that of the conformational change in each subunit. This model is typified by the schemes proposed for activation of voltage-dependent potassium channels by Zagotta and Aldrich (1990*b*) and Koren, Liman, Logothetis, Nadal, and Hess (1990). Class C represents a more general version of class B. In this class of models the concerted opening conformational change does not absolutely require the conformational changes in each subunit, but is simply promoted by them. This model is reminiscent of the mechanism of allosteric interactions in hemoglobin proposed by Monod, Wyman, and Changeux (1965) and has also been suggested as a model for activation of voltage-dependent calcium and potassium channels (Greene and Jones, 1993; Marks and Jones, 1992). Class D postulates that the opening of the channel requires not one, but two conformational changes within each subunit. These two different conformational changes are absolutely coupled, so that the second transition in each subunit cannot occur until the first one has occurred. Finally, class E represents a more general version of class D. In this class of models the two conformational changes occurring within each subunit are considered to be only partially coupled. This allows for the channel to undergo the second conformational change before the first. However, similar to class C models, the second conformational change might be promoted by the first.

This list of potential models in no way exhausts the possible gating schemes for activation. We have chosen to analyze these models because they provide reasonable hypotheses for the gating mechanism and because many of them have been proposed previously for other ion channels and allosteric enzymes. Their predictions will be compared with the data, with a particular emphasis on those predictions that differ among the models. Then, a model will be presented that can account for a large number of the phenomena described in the previous two papers (Hoshi et al., 1994; Zagotta et al., 1994).

Steady State P_O Versus Voltage Relations

The voltage dependence of the steady state P_O was calculated from the models as the equilibrium probability of being in the open state as a function of voltage. As indicated below, this solution may be different from what is actually measured experimentally. These equilibrium solutions depend only on the equilibrium constants for the transitions and not on the absolute magnitude of the rate constants. For any sequential model containing N sequentially numbered states, with states numbered 1 to n-1 closed and from n to N open, the equilibrium probability of being in

the open state is given by the following equation:

$$P_0(V) = \frac{\sum_{i=n}^{N}\left(\prod_{j=1}^{i} K_j\right)}{\sum_{i=1}^{N}\left(\prod_{j=1}^{i} K_j\right)} \tag{1}$$

where K_j indicates the equilibrium constant between states j-1 and j, and $K_1 = 1$. This equation can be generalized to nonsequential models if the term $\Pi_{j=1}^{i} K_j$ is defined as the product of the equilibrium constants for any pathway from state 1 to state j. Note that for a two state scheme where the equilibrium constant is exponentially dependent on voltage, Eq. 1 reduces to the following:

$$P_0(V) = \frac{K}{1+K} = \frac{1}{1+K^{-1}} = \frac{1}{1+K_0^{-1}e^{-zFV/RT}} \tag{2}$$

where K_0 is the value of the equilibrium constant at 0 mV, z is the equivalent charge movement for the transition, F is Faraday's constant, R is the universal gas constant, and T is the absolute temperature. Eq. 2 is simply a Boltzmann distribution with a midpoint at $V_{1/2} = -RT/zF \ln(K_0)$.

A class A model with four independent and identical transitions can be summarized as follows:

$$C_1 \overset{4K}{\longleftrightarrow} C_2 \overset{3K}{\longleftrightarrow} C_3 \overset{2K}{\longleftrightarrow} C_4 \overset{1K}{\longleftrightarrow} O$$

SCHEME I

where C_1 to C_4 represent closed conformations after 0 to 3 independent transitions respectively, O represents an open conformation, and K represents the equilibrium constant for each independent transition. If K is exponentially dependent on voltage, the equilibrium P_0 for Scheme I is given by a power of a Boltzmann distribution:

$$P_0(V) = \left(\frac{1}{1+K_0^{-1}e^{-zFV/RT}}\right)^n \tag{3}$$

where n is the number of independent and identical transitions.

In general, models with many states, like those in Fig. 1, exhibit a more complex equilibrium voltage dependence than a Boltzmann distribution or power of a Boltzmann distribution. However, many of these more complex voltage-dependencies can be well approximated by a power of a Boltzmann distribution. Fig. 2 *A* shows the P_0 predictions of class B models with four independent and identical voltage-dependent transitions and a final, concerted voltage-independent transition, similar to the models of Zagotta and Aldrich (1990*b*) and Koren et al. (1990). This model can be summarized as follows:

$$C_1 \overset{4K}{\longleftrightarrow} C_2 \overset{3K}{\longleftrightarrow} C_3 \overset{2K}{\longleftrightarrow} C_4 \overset{1K}{\longleftrightarrow} C_5 \overset{L}{\longleftrightarrow} O$$

SCHEME II

where L represents the equilibrium constant for the concerted voltage-independent transition and the other symbols were defined previously. The equilibrium constant of the final transition, L, was varied between 0.1 and 1,000, and the maximum P_0 was normalized to 1. As L was increased, the voltage dependence of the P_0 became steeper. However, as expected, the rate of the exponential rise at very low P_0 is unaffected by varying the equilibrium constant of the final voltage-independent transition. As pointed out by Almers (1978) (see also Andersen and Koeppe, 1992) and analyzed in the previous paper (Zagotta et al., 1994), this limiting exponential

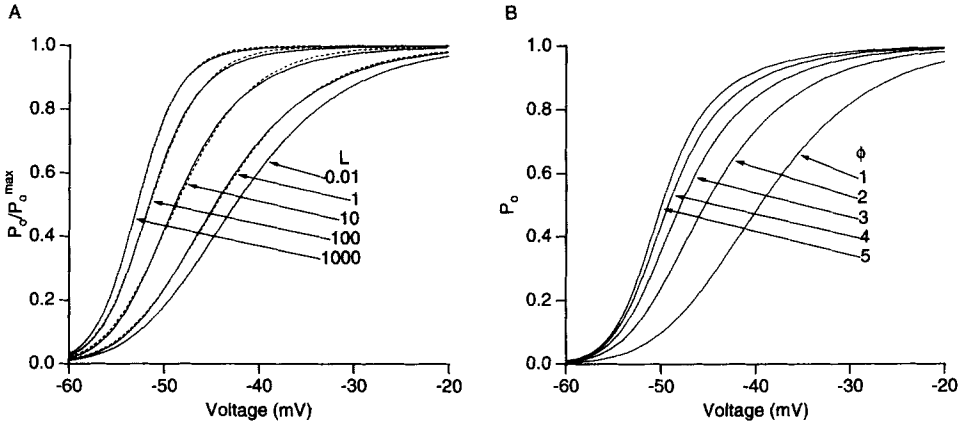

FIGURE 2. (*A*) Voltage dependence of the normalized steady state probability of the channel being open in Scheme II, a class B model with four independent and identical transitions and a final concerted transition. The open probability was calculated as described in the text with $K = K_0 e^{(3.5V/25.5)}$ where V is the membrane voltage in mV, using L = 1,000, 100, 10, 1, and 0.1 (from left to right). The resulting curves were scaled to 1. For the L = 0.1 trace, K_0 = 1,700. For all the traces where L > 0.1, the equilibrium constants at 0 mV (K_0) were adjusted so that the limiting probabilities at low Po were the same as those for L = 0.1. Powers of Boltzmann fits (see Eq. 3) are also shown superimposed as dashed lines. The total charge movement for the Boltzmann curves was held constant at z = 14. The values of the n's for the fits were (from left to right) 1.35, 1.72, 2.53, 3.55, and 3.94. (*B*) Voltage dependence of the normalized probability that the channel is open according to Scheme III, a class A model with cooperative interactions. The cooperativity was introduced as described in the text. The curves were calculated using ϕ = 5, 4, 3, 2 and 1 (from left to right). When ϕ = 1, the model is an independent model and $K = K_0 e^{(3.5V/25.5)}$ where K_0 = 1,200. For all the traces where ϕ > 1, the equilibrium constants at 0 mV (K_0) were adjusted so that the limiting probability slopes at low Po were the same as the those for ϕ = 1.

rise reflects the total equivalent charge movement, which is unaltered in the different models of Fig. 2 *A*. Each of the model predictions is fitted with a power of a Boltzmann distribution (Eq. 3) where the total equivalent charge in the fit (nz) was set equal to the total equivalent charge in the model ($4z_s$, where z_s is the charge movement associated with the conformational change in each subunit). The predictions of these class B models are clearly well described by powers of Boltzmann distributions (*dashed curves*) where n decreases as L increases. When the equilibrium of the final transition is heavily biased toward the open state, the voltage dependence of

P_0 is indistinguishable from a Boltzmann distribution, and when the equilibrium of the final transition is heavily biased toward the closed state, the voltage dependence of P_0 is indistinguishable from a forth power of a Boltzmann distribution. Therefore, even though the analytical expression for the voltage dependence of P_0 is quite complex for this model, the predicted voltage dependence is indistinguishable from Eq. 3 where the total charge movement is preserved and $1 \leq n \leq 4$. In this case the experimentally determined value of n is no longer equal to the number of transitions and may be a noninteger value.

The voltage dependence of P_0 is also made steeper at moderate P_0 by including cooperative interactions among the subunits. Cooperativity was introduced into a class A model by including an energy of stabilization for each transition that is proportional to the number of transitions that have already occurred. This model can be expressed as follows:

$$C_1 \overset{4K}{\longleftrightarrow} C_2 \overset{\frac{3}{4}K\phi}{\longleftrightarrow} C_3 \overset{\frac{2}{3}K\phi^2}{\longleftrightarrow} C_4 \overset{\frac{1}{4}K\phi^3}{\longleftrightarrow} O$$

SCHEME III

where K represents the equilibrium constant for each transition in the absence of cooperativity, and ϕ represents a cooperativity stabilization factor. Fig. 2 *B* shows the predicted voltage dependence of this model with ϕ ranging from 1 to 5. The effect of cooperativity is, once again, to increase the steepness of the voltage dependence of Po only at intermediate and high probabilities, making the voltage dependence of Po shaped more like a Boltzmann distribution. This effect is also seen when cooperativity is implemented in other ways, such as when the equilibrium constants of the four sequential transitions are the same (Vandenberg and Bezanilla, 1991), or when a stabilization factor is introduced only when a neighboring subunit has changed conformation (Hill and Chen, 1971*a;* Tytgat and Hess, 1992). In fact, a concerted final opening transition, as discussed above, or a slow first closing transition as discussed in the previous paper (Zagotta et al., 1994) also increase the steepness of the voltage dependence of P_0 at intermediate and high probabilities. Because these transitions cannot be accounted for by the independent action of multiple subunits, they also are also a form of cooperativity. Note that all of the models in Fig. 2 exhibit an identical amount of charge movement and yet the slope of the steady state P_0 versus voltage relation is dramatically altered by this cooperativity. This further illustrates the limitations of these steady state measurements in determining the charge movement.

The different models in Fig. 1 cannot be easily distinguished based on their fits to the steady state activation data. Fig. 3 *A* shows a plot of the predictions of one model from each of the classes in Fig. 1 superimposed on the P_0 vs. voltage data measured from the tail currents as described in the previous paper (Zagotta et al., 1994). Note that while these models predict subtle differences in the voltage dependence of P_0, these differences are insignificant compared to the error estimates in the P_0 vs voltage data. Therefore, by themselves, these fits cannot be used to discriminate among these classes of models as has been attempted previously (Liman, Hess, Weaver, and Koren, 1991). However, some general characteristics in the models were

necessary to produce an adequate fit for all of the models considered. All of the models require the equivalent of at least 12 to 16 total charges moving in the transitions before opening. Less charge, 12 or 13 charges, is sufficient if the model predicts a P_0 vs voltage relation described by a low power of a Boltzmann distribution (cooperative models), while more charge, at least 16 charges, is required if the P_0 vs voltage relation is described by a forth power of a Boltzmann distribution (independent models). This is also illustrated in Fig. 2 *B* of the previous paper (Zagotta et al., 1994). A second characteristic pertains to models that contain multiple types of voltage-dependent transitions, such as some class B and D models. For these models the equilibrium constant for the voltage-dependent transition occurring first, such as K in Scheme II, cannot be substantially larger than that of the transitions occurring later such as L in Scheme II. This is because if a later voltage-dependent transition

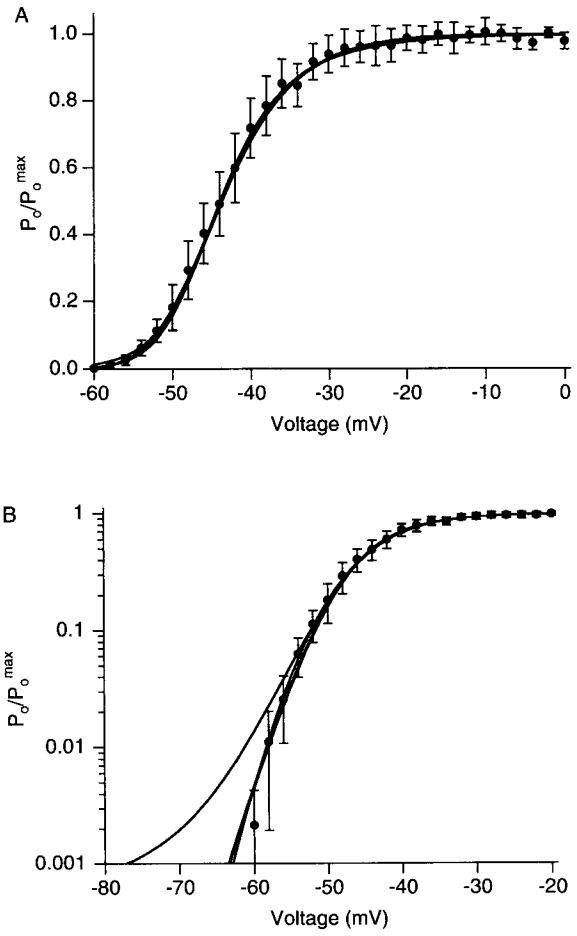

FIGURE 3. (*A*) Voltage dependence of the normalized probability that the channel is open obtained from the tail current measurements (see previous paper, Zagotta et al., 1994). The error bars indicate the standard error of the mean. Predictions of one model from each of the five classes in Fig. 1 are also shown superimposed and they are essentially indistinguishable. For the class A model (see Scheme III), K = 420 exp(V/7.8) and ϕ = 6.5. For the class B model (Scheme II), K = 440 exp(V/7.8) and L = 5. For the class C model (see Scheme IV), K = 450 $e^{(V/7.5)}$, L = 5, and f = 10. For the class D model (see Fig. 7), α/β = 3 $e^{(V/14)}$, γ/δ = 132 $e^{(V/17.6)}$ and ϕ = 9.44. Note that for these calculations, the Cf state was not included. For the class E model (see Fig. 1), the equilibrium constants for the transitions between R1 and R2, R2 and A, R1 and R3, and R3 and A were α/β, γ/δ, f* α/β, and f*γ/δ, respectively. α/β = 1,100 $e^{(V/6)}$. γ/δ = 20. f = 10. V represents the membrane voltage in mV. (*B*) The data shown in *A* are plotted as a semilogarithmic plot. The predictions of the five classes of the model essentially superimpose except for that made by the class C model.

requires much higher voltages to occur, it will dominate the voltage dependence of P_0. In fact a mechanism involving the destabilization of a second voltage-dependent transition has been proposed to account for the decreased slope of the P_0 vs voltage relation induced by a mutation near the S4 region (Schoppa, McCormack, Tanouye, and Sigworth, 1992).

The class C model used for the predictions in Fig. 3 *A* can be summarized as follows:

$$\begin{array}{ccccccccc} & & 4K & & \tfrac{3}{2}K & & \tfrac{2}{3}K & & \tfrac{1}{4}K & \\ C_1 & \longleftrightarrow & C_2 & \longleftrightarrow & C_3 & \longleftrightarrow & C_4 & \longleftrightarrow & C_5 & \\ \updownarrow & & \updownarrow & & \updownarrow & & \updownarrow & & \updownarrow & L \\ O_1 & \longleftrightarrow & O_2 & \longleftrightarrow & O_3 & \longleftrightarrow & O_4 & \longleftrightarrow & O_5 & \\ & & 4Kf & & \tfrac{3}{2}Kf & & \tfrac{2}{3}Kf & & \tfrac{1}{4}Kf & \end{array}$$

SCHEME IV

where K represents the equilibrium constant for each independent transition, L represents the equilibrium constant for the concerted transition, and f represents the factor by which the concerted transition is stabilized by each independent and identical voltage-dependent transition. The predicted P_0 vs voltage relation of Scheme IV exhibits one qualitatively different characteristic from those of the other models. At low voltages, the predicted P_0 increases less steeply with voltage. This is particularly evident in the semilog plot of the P_0 vs voltage relation shown in Fig. 3 *B*. It arises from the fact that this class of models allows the channel to open only by undergoing the concerted transition. If the concerted transition is not voltage dependent, the P_0 vs voltage relation will level off at low voltages, suggesting the channel might exhibit a small but constant open probability at any arbitrarily negative voltage. If the concerted transition is voltage dependent, the Log P_0 vs voltage relation will still become markedly less steep at negative voltages. Because this decreased slope of the Log P_0 vs voltage relation is not observed in the data, the equilibrium probability of being in state O_1 at low voltages must be extremely small. We estimate that f, the factor by which the concerted transition is stabilized by each of four independent and identical voltage-dependent transitions, must be at least 20. Therefore the only open state in Scheme IV that is likely to ever be populated is state O_5. This conclusion would also be consistent with the finding that the open times are generally described by a single exponential distribution (see first paper, Hoshi et al., 1994). With this large estimate for f, the class C model in Scheme IV is essentially identical to the class B model in Scheme III.

Activation Time Course at Depolarized Voltages

While the models could not be easily distinguished based on their steady state predictions, they make different predictions in their kinetic behavior. In this section, we will use the activation time course to discriminate among the models. The activation time course from six different patches with steps to 0 and +50 mV are normalized by their peak current amplitude and compared in Fig. 4, *A* and *B*, respectively. This figure illustrates the typical variability seen among different

patches. The time-to-half maximal currents vary by ~1 ms at 0 mV and 0.5 ms at +50 mV. The currents activate with a sigmoidal time course which, as shown in the previous paper (Zagotta et al., 1994), reflects the requirement for many conformational changes before opening. Sigmoidicity, as defined in the previous paper, reflects the number of conformational changes and their relative rates but does not

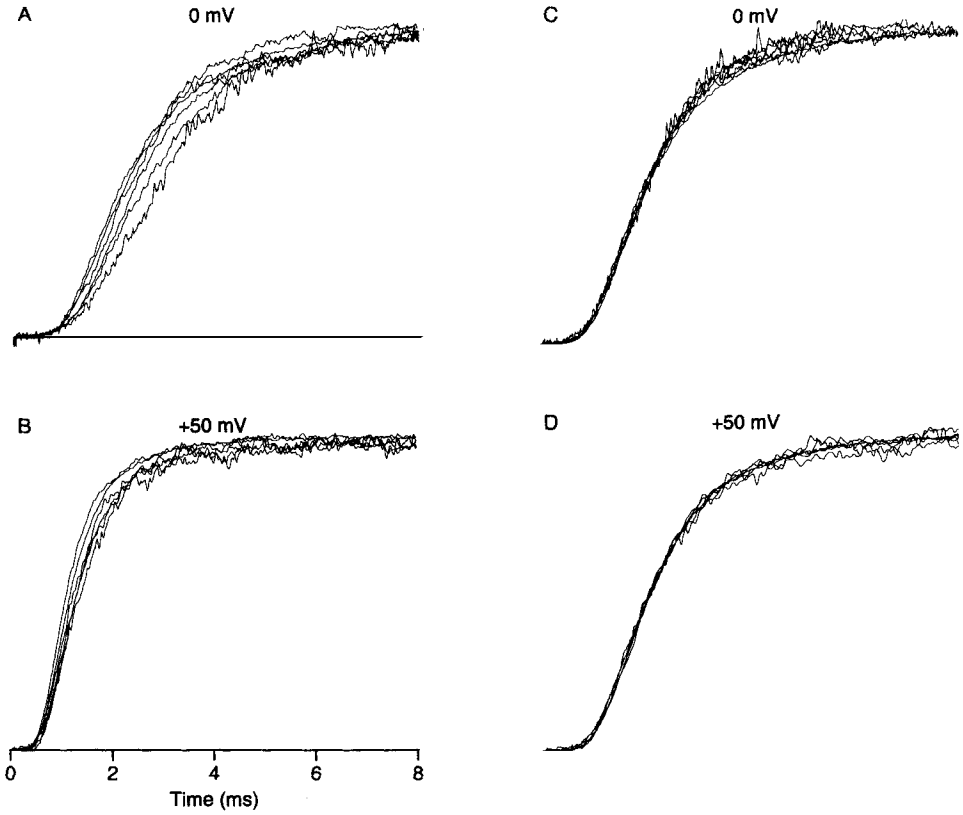

FIGURE 4. (*A* and *B*) The activation time course from six different patches at 0 mV (*A*) and at +50 mV (*B*). The currents are scaled so that their peak amplitudes are the same. The currents were elicited in response to voltage steps to 0 or +50 mV from a holding voltage of −100 mV. The data were filtered at 10 or 8 kHz. The data from five of the six patches were recorded using the standard extracellular solution described. The data from the other patch were recorded using the NMG-solution with no added K^+ used to record the gating currents. (*C* and *D*) The currents shown in *A* and *B* were scaled to compare the sigmoidicity as described in the previous paper (Zagotta et al., 1994).

depend on the absolute rate for any particular transition. As shown in the previous paper (Zagotta et al., 1994), the sigmoidicity can be seen by adjusting the time scales of the different current traces so that the rate of rise at their half maximal current is similar. As can be seen in Fig. 4, *C* and *D*, the degree of sigmoidicity varied much less between patches than the overall time course of activation. This suggests that the

currents from different patches vary primarily in the absolute rate for these transitions and not in the number of transitions or their relative rates. Because of this variability, occasionally the parameters of the model had to be adjusted to fit particular experiments.

The classes of models in Fig. 1 differ markedly in their predictions for the time course of activation with steps to depolarized voltages. In the previous paper (Zagotta et al., 1994) we showed that a minimum of six independent and identical transitions or five cooperative transitions would be required to reproduce the sigmoidal delay seen in the activation time course. However, because class A models only exhibit four transitions before opening, these models with any amount of cooperativity could never account for the observed sigmoidal delay. Class B and C models, with five transitions before opening, would only produce a sufficient sigmoidal delay if the rate of the forward transitions maintain a ratio of 1:1:1:1:1. To produce this ratio, the rate of the four identical transitions would have to increase as activation proceeds so as to exactly compensate for the decreased number of allowed transitions (Vandenberg and Bezanilla, 1991). Furthermore, because the sigmoidicity is not significantly altered up to at least +140 mV, this ratio would have to be maintained over a wide range of voltages. Therefore, the rate and voltage dependence of the concerted transition would have to be quite similar to those of the identical transitions. If the concerted transition were voltage independent, as in the model of Zagotta and Aldrich (1990*b*), it would become rate limiting at large depolarized voltages and result in a significant loss in the sigmoidicity in the activation time course (Schoppa, McCormack, Tanouye, and Sigworth, 1991). These restrictions on the rates of the class B and C models are inconsistent with the results of reactivation and the effects of holding voltage on the activation kinetics (see previous paper, Zagotta et al., 1994). Therefore class *A, B* and *C* models could never completely account for all of the data presented in the previous paper.

Class D and E models both require a minimum of eight transitions before opening, two in each subunit. In this respect, both models are quite capable of producing the sigmoidal delay seen in the activation time course. To estimate the forward rates for these models, we have fitted the activation time courses at depolarized voltages with the predictions of a scheme involving the independent action of four subunits, each of which must undergo two coupled transitions to open the channel. This scheme can be abbreviated as follows:

$$\left[R_1 \overset{\alpha}{\rightarrow} R_2 \overset{\gamma}{\rightarrow} A\right]^4$$

SCHEME V

where α and γ represent the rate constants of the first and second forward transitions respectively, R_1 and R_2 represent resting states and A represents the activated state for each subunit. When all four subunits are in the A state the channel is considered to be open. The rates of the reverse transitions are expected to be small at depolarized voltages and so were ignored. The fits of Scheme V to the activation time course with steps to between 0 and 50 mV is shown in Fig. 5 *A*. The rates that

produced these fits and those from other patches are plotted as a function of voltage in Fig. 5 *B*. Note that both rates increase with voltage with a roughly similar voltage dependence. This is expected because a similar voltage dependence will maintain a constant ratio between the rates, and therefore a constant sigmoidicity in this voltage range as required by the data. Single exponential functions were fitted to the voltage dependencies of the rates and are superimposed on the data in Fig. 5 *B*. One of the

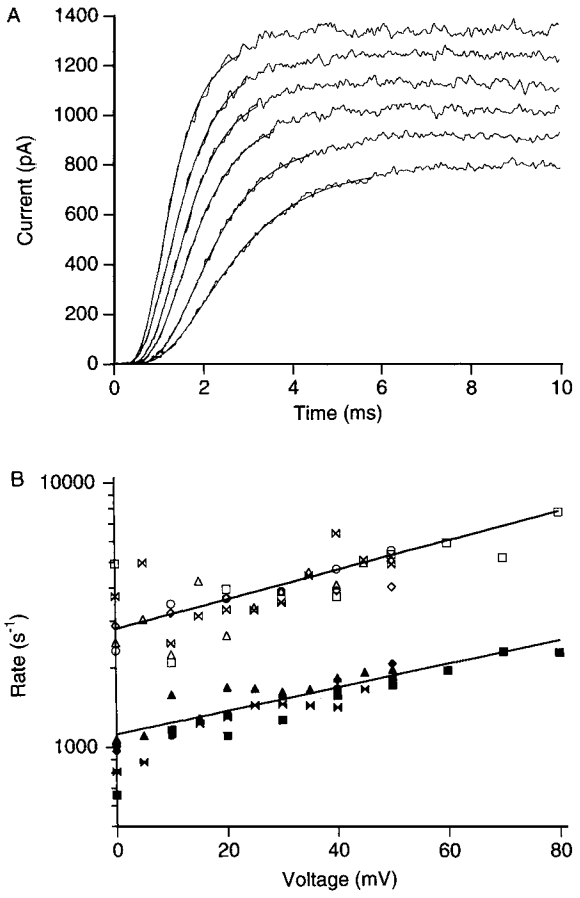

FIGURE 5. (*A*) The fits of Scheme V (see the main text) to the activation time course. The currents were elicited in response to voltage pulses to between 0 and +50 mV from a holding voltage of −100 mV. The data were filtered at 10 kHz and digitized every 20 μs. The backward rates were assumed to be zero. All the subunits are set to be in R_1 at t = 0. The fits were done on the data points up to 90% of the peak amplitudes because the very late phase of the activation time course was variable among the experiments. (*B*) Voltage dependence of the two forward rate constants in Scheme V. The ionic currents from five different patches were fitted with Scheme V. Values of the two forward rate constants are plotted and fitted with exponential functions. For the fastest rate constant (*unfilled symbols*), its value at 0 mV was 2,800/s and the equivalent charge was 0.32 electronic charges. For the other rate constant, they were 1,140/s and 0.25 electronic charges.

rate constants is 1,140 s^{-1} at 0 mV and increases e-fold per 100 mV, corresponding to an equivalent charge movement of 0.25 electronic charges. The other rate is ~2,800 at 0 mV and increases e-fold per 80 mV, corresponding to an equivalent charge movement of 0.32 electronic charges. The solution to Scheme V is identical whether the faster rate corresponds to α or γ. Nevertheless, as will be shown later, these different orientations of the rates predict very different gating current time courses.

Deactivation Time Course and Voltage Dependence

In the preceding discussion, we have analyzed the implications of the activation time course at depolarized voltages on the rates and voltage dependence of the forward transitions in the various models. In this section we analyze the implications of the deactivation time course on the reverse transitions in the models. The deactivation time course from seven different patches with repolarizing steps to −80 and −40 mV are normalized by their peak current amplitude and compared in Fig. 6, *A* and *B*, respectively. This figure illustrates the typical variability in deactivation time course

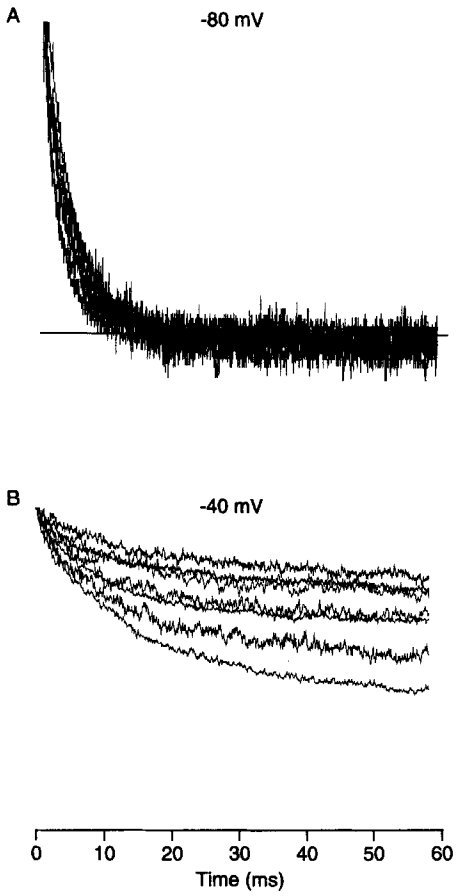

FIGURE 6. The deactivation time course from seven different patches at −80 mV (*A*) and at −40 mV (*B*). The currents were scaled to the instantaneous current amplitudes immediately after the depolarizing pulses. The patches were depolarized to +50 mV for 10 ms and then to −80 mV (*A*) or −40 mV (*B*). The data were filtered at 3 to 6 kHz and digitized every 34 μs.

seen in different patches. Note that the tail currents at −80 mV were much more reproducible than those at −40 mV. This occurs because the channels are about 70% activated at −40 mV and the steady state activation is steeply dependent on membrane voltage. Therefore small differences in the voltage dependencies in different patches (±5 mV) will cause large differences the steady state level of the tail currents. At −80 mV, however, much less variability is seen because the steady-state

level of activation is virtually zero. Because of this variability, occasionally the parameters of the model had to be adjusted to fit particular experiments.

The deactivation time course at hyperpolarized voltages is dominated by the transitions near the open state and has been examined both at the macroscopic and single-channel level. In the previous paper (Zagotta et al., 1994), it was found that macroscopic deactivation at hyperpolarized voltages (−160 to −50 mV) exhibits a nearly single exponential time course with a time constant that decreases e-fold per 24 mV of hyperpolarization. From the analysis of single-channel currents in the first paper (Hoshi et al., 1993), this deactivation was found to reflect more than just the rate of the closing transition. Upon hyperpolarization, the channels opened and closed in bursts before entering an absorbing closed conformation. Both the burst durations and the open durations decreased with increasing hyperpolarizations. The voltage-dependence of the open durations and total open time during a burst suggested that the channel can undergo at least two types of closing transitions, as shown in the partial kinetic scheme below:

$$\ldots C \overset{\Delta V}{\longleftarrow} O \longleftrightarrow C_f$$

SCHEME VI

where $\ldots C$ represents closed states in the activation pathway and C_f represent a shorted-lived closed state. Closures to C_f occurred with a rate that was virtually voltage-independent and were the predominant closures seen at depolarized voltages. Closures to $\ldots C$ occurred with a rate that increased exponentially with hyperpolarization, ~e-fold per 22 mV of hyperpolarization. The voltage-dependent closing transition becomes appreciable at hyperpolarized voltages and accounts for the voltage dependence of the macroscopic deactivation.

Class A and B models as shown in Fig. 1 contain only one closing transition. To account for the voltage-dependence of the open durations and total open time during a burst, these models would have to be extended to include closures to states not directly in the activation pathway. This is summarized for a class A model in the scheme below:

$$C_1 \overset{\Delta V}{\longleftrightarrow} C_2 \overset{\Delta V}{\longleftrightarrow} C_3 \overset{\Delta V}{\longleftrightarrow} C_4 \overset{\Delta V}{\longleftrightarrow} O \longleftrightarrow C_f$$

SCHEME VII

where C_f represents a closed conformation not directly in the activation pathway. In Scheme VII the $O \rightarrow C_f$ rate is voltage-independent while the $O \rightarrow C_4$ rate increases e-fold per 22 mV, corresponding to 1.16 electronic charges moving between the open state and the transitions state to closing. From the analysis in the previous paper (Zagotta et al., 1994), it was estimated that the voltage dependence of the forward transitions corresponds to ~0.4 electronic charges moving between the closed state and the transition state to opening. Taken together, Scheme VII would contain only 1.6 electronic charges moving for each subunit or a total of only 6.4 electronic charges moving for the activation transitions. This is significantly less than the 12 to 16 electronic charges estimated for the activation transitions from the voltage

dependence of the steady state probability of being open, and once again demonstrates that class A models are not adequate to account for channel activation.

These problems are partially alleviated by the class B model summarized below:

$$C_1 \overset{\Delta V_1}{\longleftrightarrow} C_2 \overset{\Delta V_1}{\longleftrightarrow} C_3 \overset{\Delta V_1}{\longleftrightarrow} C_4 \overset{\Delta V_1}{\longleftrightarrow} C_5 \overset{\Delta V_2}{\longleftrightarrow} O \longleftrightarrow C_f$$

SCHEME VIII

where ΔV_1 represents the voltage-dependence of the transition within each subunit and ΔV_2 represents the voltage-dependence of the concerted transition. This model has previously been proposed to account for the gating currents in *Shaker* channels with a mutation near the S4 segment (Schoppa et al., 1992). To fit the voltage dependence of the steady state open probability and the deactivation kinetics with Scheme VIII, the concerted transition could move 1.6 electronic charges and each of the transitions within each subunit could move 2.6 to 3.6 electronic charges. However, in addition to not producing enough sigmoidal delay, Scheme VIII cannot account for the time course of the OFF gating currents for channels that have not yet opened, as shown below.

The class C models provide a different interpretation of the deactivation transitions. Because this class of models contains multiple open states, the measured closing rates would represent a weighted sum of the closing rates from each of the open states. Furthermore, the closing rates from the lower open states, such as O_4 and O_3 in scheme IV, would be expected to be faster than from O_5. If the concerted transitions were voltage-independent, the open times would be voltage independent at depolarized voltages where the channels could close predominantly from O_5, and would decrease at more hyperpolarized voltages, where the channels would close more frequently from the lower open states. The class C models, therefore, quite naturally account for the nonexponential voltage-dependence of the open times without invoking a closed state not in the activation pathway. However, as mentioned earlier, these models would predict multiple components to the open time distribution, which were not observed. In addition, the large value of f estimated from fits to the P_0 vs voltage relation might preclude the occurrence of the lower open states at only moderately hyperpolarized voltages.

The class D and E models both contain a second transition in each subunit that is required for channel opening. However the class D model as shown in Fig. 1 contains only one closing transition. As for class A and B models, this model would have to be extended to include closures to states not directly in the activation pathway to account for the voltage-dependence of the open durations and total open time during a burst. The class E models afford a simple explanation for the nonexponential voltage-dependence of the open times. In these models the open channel can close in either of two ways, by the reverse of the first transition or by the reverse of the second transition. If the second transition is voltage-independent, the open times would be voltage independent at depolarized voltages, where the channels would close by the second transition, and would decrease at more hyperpolarized voltages, where the channels would close by the voltage-dependent first transition. However, as for class A models, the voltage dependence of the reverse of the first transition is not

adequate to account for the total voltage dependence of activation. Therefore, for these models, it seems likely that both transitions of each subunit would have to carry a significant amount of charge, as already suggested for the voltage-dependence of the forward transitions in Fig. 5.

ON Gating Current Time Course

The rate of the transitions among closed states away from the open state can be investigated by analyzing the time course of the ON gating currents. As shown in the previous paper (Zagotta et al., 1994), the gating currents above −20 mV exhibit a small rising phase or plateau followed by an exponential decay. It has been shown that a rising phase of the ON gating currents can arise as an artifact in the protocol to subtract linear capacitance (Armstrong and Bezanilla, 1974; Stuhmer, Conti, Stocker, Pongs, and Heinemann, 1991). However, we have observed a similar rising phase with several different subtraction protocols (see methods in previous paper [Zagotta et al., 1994]) and therefore believe that it did not arise entirely from improper subtraction of linear capacitance. This rising phase has often been interpreted to indicate nonindependent, or cooperative, gating among the subunits during the activation transitions (Perozo, Papazian, Stefani, and Bezanilla, 1992; White and Bezanilla, 1985). The time course of these gating currents can be approximated by a class A, B, or C model where the relative rates of the forward transitions in each subunit are adjusted so that a slower voltage-dependent transition is followed by more rapid voltage-dependent transitions (Perozo et al., 1992). Even without cooperative interactions among subunits, class D and E models can exhibit a rising phase of the ON gating current, as shown for a class D model later. Alternatively, a rising phase of the ON gating currents can be produced by a more weakly voltage-dependent transition followed by a more strongly voltage-dependent transition.

OFF Gating Current Time Course

The rate of the reverse transitions among closed states away from the open state can be investigated by analyzing the time course of the OFF gating currents at hyperpolarized voltages for channels that have not been allowed to reach the open state. As shown in the previous paper (Zagotta et al., 1994), this rate can be estimated by measuring the OFF gating currents after short pulses to +50 mV or after longer pulses to between −60 and −20 mV. Both methods produce OFF gating currents at −100 mV with roughly a single exponential time course with a time constant of ~0.5 ms. This indicates that the rate limiting step for return of the gating charge in channels that have not yet opened is ~2,000 s^{-1} at −100 mV, markedly faster than the rate of closure of open channels (about 1000 s^{-1} at −100 mV in our standard solution).

A rate of 2,000 s^{-1} at −100 mV, however, is much slower than is expected for class A, B, and C models based on the steady-state properties discussed earlier. If many of the transitions before opening represent single independent and identical transitions in each subunit, as in class A, B, and C models, the rate of these OFF gating currents is a direct measure of the rate of the reverse transition for each subunit. As shown in Fig. 3, the class A model in Scheme I can quite readily account for the steady state P_0

vs voltage data. The equilibrium constant, K, for the elementary transition in this model is given by the following equation:

$$K = \frac{\alpha}{\beta} \tag{4}$$

where α is the rate of the forward transition and β is the rate of the reverse transition in each subunit. K was assumed to be exponentially dependent on voltage with $K_{-100} = 0.0011$. α was estimated in the previous paper (Zagotta et al., 1994) to be $\sim 1{,}000\ s^{-1}$ at 0 mV and increased e-fold per 60 mV. Extrapolation of this estimate down to -100 mV gives $\alpha_{-100} = 190\ s^{-1}$. Substitution of K_{-100} and α_{-100} into Eq. 4 gives $\beta_{-100} = 1.7 \times 10^5\ s^{-1}$. Note that this predicted value of β_{-100} is significantly faster than the rate of $2{,}000\ s^{-1}$ measured from the OFF gating currents. Furthermore, for class B and C models, Schemes II and IV respectively, the equilibrium constant for the concerted conformational change, L, is generally greater than K, resulting in an even greater predicted value for β_{-100}. While we cannot rule out the possibility that the extrapolations for estimating K_{-100} and α_{-100} from more depolarized voltages may be in error, this error would have to be quite significant to account for the large discrepancy between the predicted and measured values of β_{-100}. This analysis suggests that, relative to independent and identical transitions, the gating charge is slowed in its rate of return even before the channel opens, and becomes even further slowed after opening. This behavior might be explained by adding cooperativity for the subunit transition in class A, B, or C models, however, as shown below, is more naturally accounted for by class D models.

A Class D Model Can Account for Most of the Channel Behavior

For a model to be successful it must be able to simultaneously fit the data from a number of different types of experiments. While class A, B and C models in Fig. 1 can be made to fit many individual steady state or kinetic experiments, the same set of rate constants cannot simultaneously fit all of these data. If the rate constants are constrained to fit the voltage-dependence of steady state activation, then these models cannot adequately account for many of the kinetic measurements, including the following: (*a*) the sigmoidal delay in the activation time course; (*b*) the voltage dependence of deactivation; (*c*) and the time course of the gating currents for channels that have not yet opened. As we have discussed above, however, models with two voltage-dependent conformational changes, classes D and E, are well suited to explain these data. In this section, we will present a class D model that can account for virtually all of the steady state and kinetic behavior that we have discussed.

A model that is consistent with the data is a class D model in which the channel requires two voltage-dependent conformational changes in each of its subunits to open and, once open, can undergo a transition to the relatively unstable closed conformation C_f. This model is summarized in Fig. 7 in both an abbreviated and more complete form and is outlined in more detail in the appendix. The gating of the different subunits is considered to be independent except for the C_f state and a slower first closing transition. The first closing transition is slowed by the factor θ. If each rate constant is assumed to be exponentially dependent on voltage, this model possesses nine free parameters for the transitions occurring before opening. The

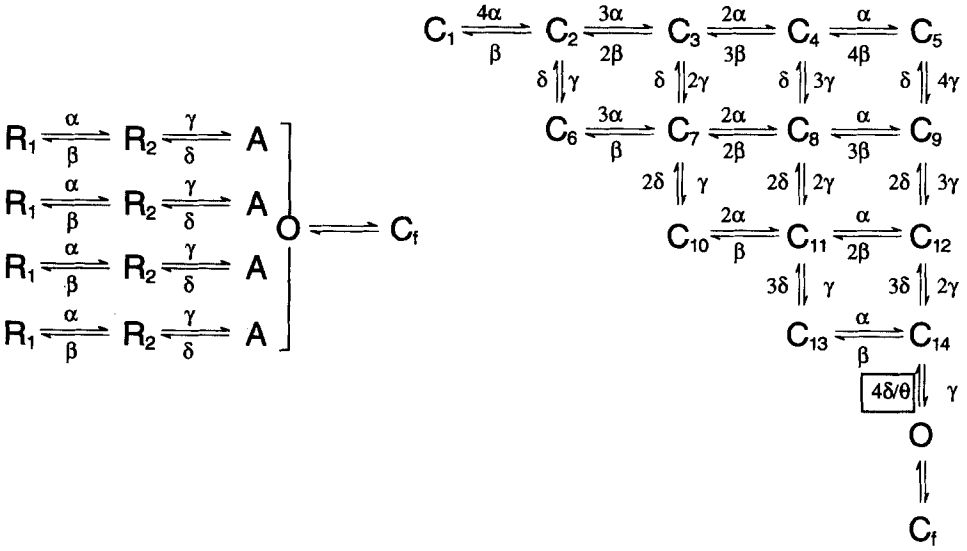

FIGURE 7. A class D model consistent with the experimental data. The model is shown in an abbreviated form (*left*) showing conformational changes of each of the four subunits, and in a complete form (*right*) showing the conformational changes in the channel.

values of these parameters that produce acceptable fits were ascertained from the data discussed above and are presented in Table I. The P_0 vs voltage relation established the total voltage dependence of the transitions and the voltage at which half of the channels were open. The rate and voltage dependence of the forward transitions were estimated from the time course of activation at depolarized voltages (Fig. 5). The rate and voltage dependence of the reverse transition out of the open state were estimated from the time course of deactivation. Finally, the time course of the OFF gating currents for channels that have not opened, estimated from short or low voltage pulses, established the value of θ.

In addition, the model contains three free parameters for the transitions after opening, the $O \rightarrow C_f$ rate, the $C_f \rightarrow O$ rate, and the voltage dependence of the $C_f \rightarrow O$ rate (the $O \rightarrow C_f$ rate was considered to be voltage-independent). These parameters were determined from an analysis of the single-channel kinetics as discussed in the

TABLE I

Summary of the Rate Constants for the Model in Fig. 7

Rate constant	k_o	z_k
k	s^{-1}	e^- *charges*
α	1120	0.25
β	373	1.6
γ	2800	0.32
δ	21.2	1.1
$O \rightarrow Cf$	600	0
$Cf \rightarrow O$	3800	0.17

The variables are defined in the Appendix. The value of θ is 9.4.

first paper (Hoshi et al., 1994). While in the first paper we suggested that the $C_f \rightarrow O$ rate had very little voltage-dependence, we find that a slight voltage dependence (e-fold per 150 mV, corresponding to 0.17 electronic charges) provides a possible explanation for the difference in the P_0 vs voltage relation measured from pulse and tail current data. This degree of voltage dependence is consistent with the fast component of the closed durations (see Fig. 9).

Steady state P_0. The equilibrium estimate of P_0 vs voltage for this model produces a nice fit to the steady state P_0 vs voltage data, as shown in Fig. 3. For this fit to the steady state P_0 vs voltage data measured from tail currents, the C_f state has been omitted for the reason discussed below. In the previous paper (Zagotta et al., 1994) we have estimated the steady state P_0 in two ways: from the current during a depolarizing voltage pulse and from the tail current after the voltage pulse. These two measurements yielded somewhat different estimates for the steady-state P_0 vs voltage relation. We suggested that the difference may be due, in part, to an error in the estimate of the single-channel current at the hyperpolarized voltages. Here, we suggest the alternative explanation that a small voltage dependence in the $Cf \rightarrow O$ transition can account for most or all of the difference. Fig. 8 *A* shows the probability time course calculated for the model in Fig. 7 using a similar pulse protocol to that used to generate the steady state P_0 vs voltage data. Measurements of the probability at the end of the first pulse, and 0.5 ms after the beginning of the tail pulse were normalized to the probabilities at 0 to 50 mV and plotted against the first pulse voltage in Fig. 8 *B*, along with the experimental data measured in a similar manner. Notice that, like the experimental data, the calculated probabilities at the end of the first pulse exhibit a shallow increase at more depolarized voltages that is not present in the calculated probabilities 0.5 ms after the beginning of the tail pulse. The difference results from a dependence of the early time course of the tail currents on the pulse voltage. The small voltage dependence to the equilibrium between the open state and C_f would produce a small increase in the P_0 measured from the pulse currents at depolarized voltages. This small increase would not be present in the P_0 measured from the tail currents because of a rapid equilibration between the open state and C_f during the tail currents. This explanation suggests that the steady state P_0 vs voltage relation measured from the pulse represents the equilibrium distribution of the entire model, while the steady state P_0 vs voltage relation measured from the tails reflects the equilibrium distribution of the model excluding the C_f state. Consistent with this suggestion, the equilibrium distribution of the model without the C_f state provides a good fit to the steady state P_0 vs voltage data measured from tail currents (Fig. 3).

Single-channel properties. The single-channel behavior is adequately described by the model in Fig. 7. The addition of the Cf state after opening predicts a partial kinetic scheme for transitions around the open state much like Scheme VI. Therefore, the distribution of open durations will be single exponential with a time constant that is nearly voltage-independent at depolarized voltages and decreases at hyperpolarized voltages. The predicted distributions were corrected for missed closed events by the method of Blatz and Magleby (Blatz and Magleby, 1986 see Hoshi et al., 1994) and superimposed on the distributions of open durations between −90 and +50 mV in Fig. 9 *A*. The open durations at −90 mV were measured in the presence

of 140 mM K^+ in the external solution to permit single-channel openings to be visualized at these hyperpolarized voltages. The predicted distributions of open durations accurately describes the nearly voltage-independent open durations between −50 and +50 mV, where the closing transitions $O \rightarrow C_f$ are dominant. Below −50 mV, the decrease in the open durations seen in the data is reproduced in the model because the voltage-dependent closing rate $4\delta/\theta$ becomes appreciable at hyperpolarized voltage.

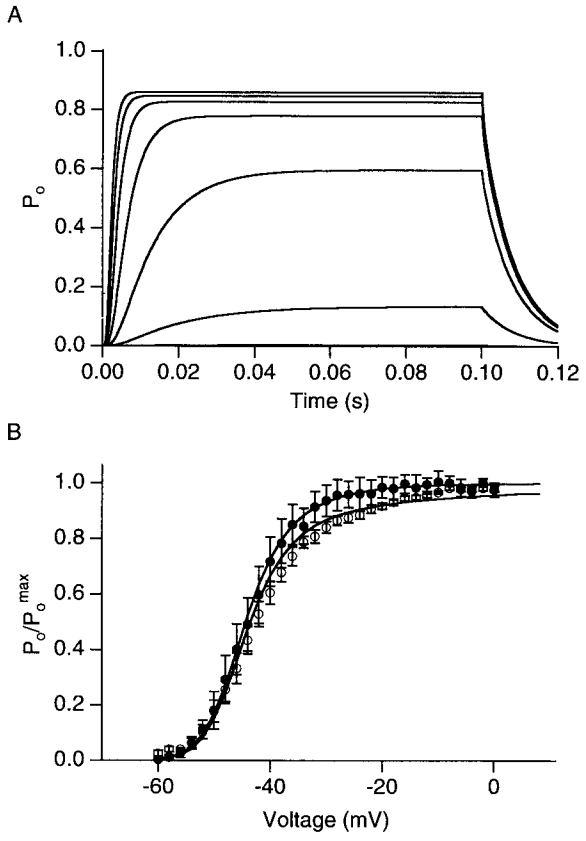

FIGURE 8. (*A*) The time course of the probability that the channel is open simulated by the model shown in Fig. 7. The model parameter values were set as in Table I. (*B*) Voltage dependence of the experimentally observed and simulated normalized open probability. The observed values were obtained as described in the previous paper (Zagotta et al., 1994). The filled symbols were obtained from the tail currents measurements and the unfilled symbols were from the peak current measurements during the pulse. The smooth curve fitted to the pulse data was measured from the open probabilities of the simulated currents in *A* during the depolarizing pulse. The smooth curve fitted to the tail data was measured from the open probabilities of the simulated currents in *A*, 0.5 ms after the depolarization pulse. Both of the open probability vs voltage curves from the model were normalized to one at +50 mV.

Fig. 9 *B* shows the distribution of closed durations for the model, after correction for missed events, compared to the data between −40 and +50 mV. As discussed in the first paper (Hoshi et al., 1994), the distribution of closed durations at depolarized voltages contains at least two exponential components, one with a fast time constant (~0.3 ms) and one with an intermediate time constant (~3 ms). The fast component of the closed durations in the model is determined from the weakly voltage dependent $C_f \rightarrow O$ rate and provides a reasonable description of the data. However, the model does not exhibit a significant intermediate component, particularly at depolarized voltage. In the first paper (Hoshi et al., 1994) we argued that this

intermediate component must arise, in part, from a closed state, designated C_i, that is not always traversed in the process of activation. While the model in Fig. 7 contains many closed states that are not always traversed in the process of activation, the characteristic closed durations produced by these states at depolarized voltages are

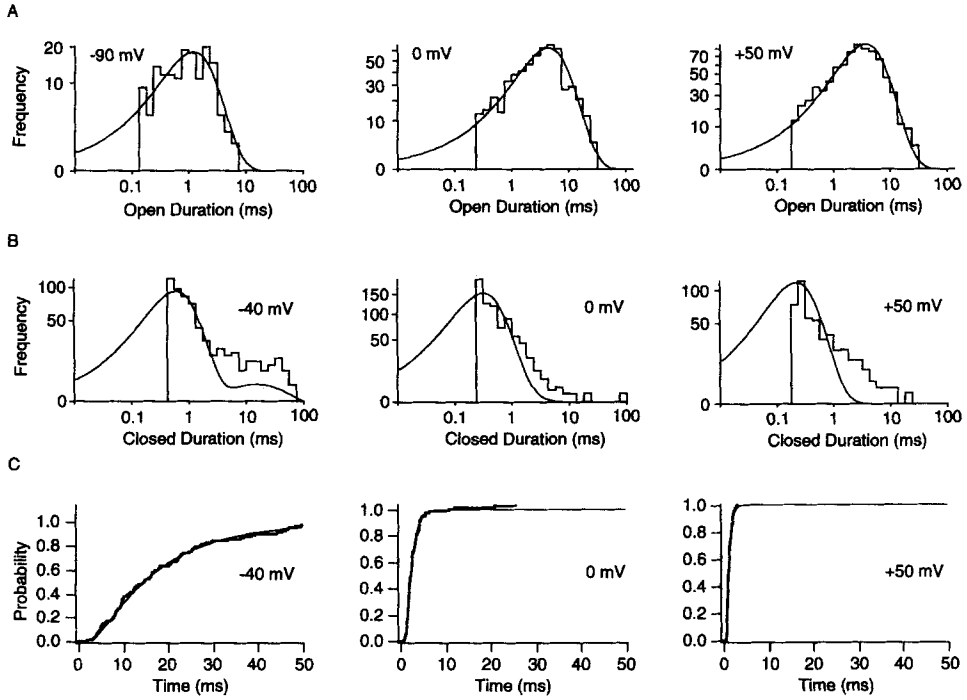

FIGURE 9. (*A*) Comparison of the observed open duration distributions and those predicted by the model in Fig. 7. The model parameter values were set as in Table I. The single-channel data were obtained as described earlier (Hoshi et al., 1994). The openings at 0 and +50 mV are obtained from the same patch using the standard low K^+ external solution. The histogram at −90 mV was obtained from the tail openings in the presence of 140 mM K^+ in the external solution. The smooth lines represent the model predictions using the above parameters with the corrections for missed events as described by Blatz and Magleby (1986). (*B*) Comparison of the observed closed durations and those predicted by the model shown in Fig. 7. The experimentally observed values were obtained as described in *A*. The model parameter values were set as in Table I. The smooth lines represent the model predictions for the closed durations after correction for missed events (Blatz and Magleby, 1986). (*C*) Comparison of the observed first latency distributions (*thick lines*) and those predicted by the model (*thin lines*) shown in Fig. 7. The observed first latencies were obtained as described (Hoshi et al., 1994). The measured first latency distributions were scaled to correct for the small number of the sweeps which failed to elicit any opening because inactivation was outside of the scope of the model.

all considerably smaller and more voltage-dependent than the intermediate component of the distribution of closed durations. Therefore, the C_i state is likely to be distinct from any of the closed states in the model of Fig. 7, and therefore closures from the Ci state are not present in the calculated distributions. Transitions to the C_i

state might occur from the C_f state or directly from the open state. The channel might additionally enter the C_i state from one of the other closed states in the activation pathway. Because closures with an intermediate duration were relatively infrequent compared to the rapid closures to the C_f state, and because of uncertainty in the coupling of the C_i state or states to the other states, we have not included C_i in the model of Fig. 7.

The model also fits the distributions of first latencies between −40 and +50 mV, as shown in Fig. 9 *C*. The relative absence of very short latencies in both the data and the model is indicative of the requirement for many conformational changes before opening. In addition, the model accurately reproduces the decrease in the first latencies with increased depolarization due to the voltage dependence of the conformational changes in the activation pathway.

Macroscopic activation. The model in Fig. 7 also provides good fits to the macroscopic activation time course over a wide voltage range. Fig. 10 *A* plots the fits to the activation time course during steps to voltages between −50 and +50 mV on a fast time scale. To fit these macroscopic currents, the probability time courses calculated from the model were multiplied by a driving force term that increased linearly with voltage and reversed at −75 mV. While this reversal potential is more positive than the Nernst potential for potassium (−110 mV), it provides a good estimate of the single-channel current amplitude between −40 and +50 mV. Fig. 10 *B* shows the fits between −50 and −20 mV on a slower time scale. Because of a nonlinear open channel current-voltage relation in this voltage range, these calculated currents were individually scaled to fit the corresponding data. The model is not only able to reproduce the voltage-dependence of the activation time course, but is also able to reproduce the large decrease in sigmoidicity at hyperpolarized voltages. In the previous paper (Zagotta et al., 1994), this decrease in sigmoidicity was shown by scaling the current levels and the time scales of the different macroscopic activation time courses so that the rates of rise of the currents at half maximal amplitude were equal. Fig. 10 *C* shows the results of this normalization procedure on the model predictions for voltage steps to −50, −40, 0, +50, and +100 mV. The sigmoidicity is significantly less at −50 and −40 mV than at depolarized voltages, and the sigmoidicity is unchanged between 0 and +100 mV. These predictions are directly comparable to the results shown in Figs. 13 and 14 of the previous paper (Zagotta et al., 1994).

Macroscopic deactivation. The model provides reasonable fits to the time course of deactivation at hyperpolarized voltages. Deactivation was measured from tail currents during hyperpolarized steps to voltages between −40 and −120 mV after 10 ms pulses to +50 mV. In Fig. 11, the tail currents were scaled and overlaid on the model predictions calculated using the same pulse protocol. The model reproduces the general time course and voltage dependence of the deactivation. However, the tail currents appeared to have a more double-exponential time course than the model predicts. The double exponential deactivation time course can arise in part from the closed state C_i, discussed in Hoshi et al., (1994), which is not present in the model of Fig. 8. In addition, the model predicts a small rapid component in the tail currents that would generally be too fast to observe experimentally. This results from the rapid relaxation of the equilibrium between the open state and C_f due to a small

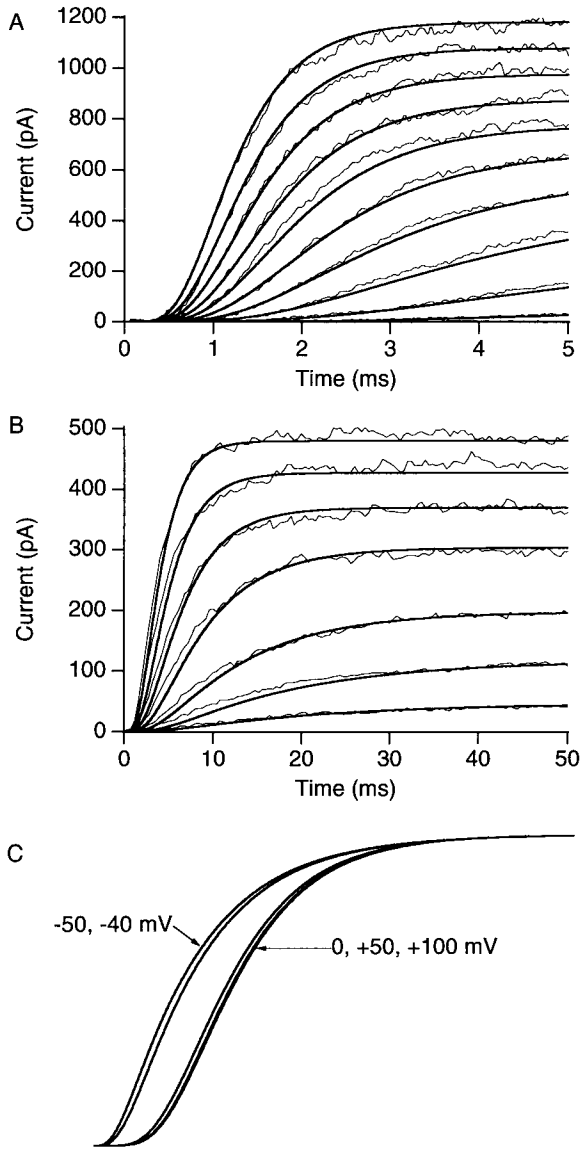

FIGURE 10. (*A*) Comparison of the observed activation time courses and those predicted by the model shown in Fig. 7. The currents were elicited in response to voltage pulses to between −50 and +50 mV in increments of 10 mV from a holding voltage of −100 mV. The data were filtered at 10 kHz and digitized every 10 μs. To calculate the open probability curves, the probability of being in C_1 was set to 1.0 at time $t = 0$. A linear single-channel current-voltage relationship ($i(V)$) with the reversal voltage of −75 mV was assumed. (*B*) Comparison of the observed activation time courses at −50 to −20 mV and those predicted by the model in Fig. 7. The currents were elicited in response to voltage pulses to between −50 and −20 mV in increments of 5 mV from a holding voltage of −100 mV. The simulated currents were scaled to match the experimentally observed currents because of the nonlinear $i(V)$ in this voltage range. The data were filtered at 1 kHz and digitized every 400 μs. (*C*) Sigmoidicity of the ionic current time course predicted by the model in Fig. 7. The currents at −50, −40, 0, +50, and +100 mV were simulated and normalized to compare the sigmoidicity as described in the main text and also in the previous paper (Zagotta et al., 1994).

amount of voltage-dependence in the $C_f \rightarrow O$ transition. This phenomenon was suggested above to be responsible for the differences in the P_0 vs voltage relations measure from the pulse current and from the tail current.

Gating currents. Fig. 12*A* shows the fits of the model to the gating currents during steps to voltages between −80 and +40 mV followed by steps to −100 mV.

Both the ON and OFF gating currents have been scaled by a constant factor equivalent to the number of channels in the patch. The general time course of the ON gating currents is well described by the model. In particular, the model predicts a rising phase in the ON gating currents with 8-ms steps to voltages above −20 mV. The predicted rising phase has a similar time course and voltage dependence to that seen in the data. A rising phase has often been interpreted to indicate nonindependent, or cooperative, gating among the subunits during the activation transitions. However, in this model, it is arising from multiple voltage-dependent transitions occurring in a single subunit. The nonindependence imposed by the slower first closing transition has virtually no effect on the ON gating currents at depolarized voltages. The steady state charge movement was estimated by integrating the ON gating currents for 16 ms after subtracting off any apparent steady state current at 16 ms. The data, normalized to the charge movement at depolarized voltages and averaged from 19 patches, are plotted as a function of voltage and compared to the model predictions in Fig. 12 *B*. The model provides a good description of the voltage dependence of the steady state charge movement.

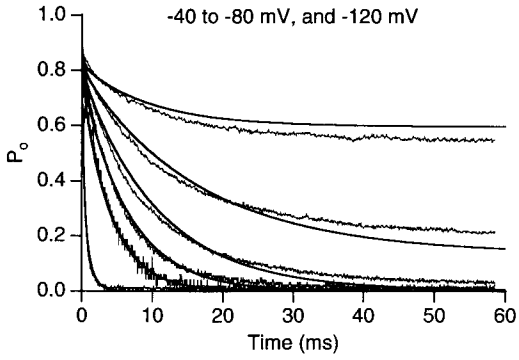

FIGURE 11. Comparison of the observed deactivation time course and the predictions of the model in Fig. 7 (*smooth curves*). The tail currents were recorded at −40, −50, −60, −70, −80, and −120 mV (from right to left) after 10 ms pulses to +50 mV. The data were filtered at 6 kHz and digitized every 34 μs. The data were scaled to fit the model's prediction for decays in the open probability.

The amplitude and voltage dependence of the forward transitions were determined from the time course of activation at depolarized voltages using fits of Scheme V. One of the rates was 1,000 at 0 mV and increased e-fold per 100 mV, whereas the other rate was 2,800 at 0 mV and increased e-fold per 80 mV. However, which rate corresponded to α and which corresponded to γ was not determined because the solution to Scheme V depends identically on α and γ. Fig. 13 *A* shows the voltage dependence of the macroscopic activation time course for the model in Fig. 7, where the slower rate corresponds to the first transition in each subunit, and for a model where the α and γ rates have been reversed. Changing the orientation of the α and γ rates necessitated changing the amplitude of the reverse rates as well to maintain fits to the steady state P_0 vs voltage relation. As expected, these two models predict a very similar activation time course and voltage dependence, especially at depolarized voltages. Nevertheless, they predicted very different gating current time courses. Fig. 13 *B* shows the predicted ON gating currents for the model in Fig. 7, as already shown in Fig. 12 *A*, while Fig. 13 *C* shows the predictions for the model where the α and γ rates have been reversed. Reversing the α and γ rates results in gating currents

that are much faster and devoid of a rising phase. Clearly these currents would not fit the data in Fig. 12 *A*, and the orientation of the rates shown in Fig. 7 is preferable.

The model in Fig. 7 also fits the OFF gating currents and their dependence on the voltage and duration of the depolarizing pulse. To fit the time course of the OFF gating currents for channels that have reached the open state the value of θ had to be altered somewhat to account for the slower deactivation kinetics in the gating current solutions as discussed in the previous paper (Zagotta et al., 1994). After 8-ms pulses to voltages below −20 mV, both the data and the model exhibit larger and faster OFF gating currents, resulting from channels that have not reached the open state (Fig. 12 *A*). The model predicts a very rapid component to these off gating currents

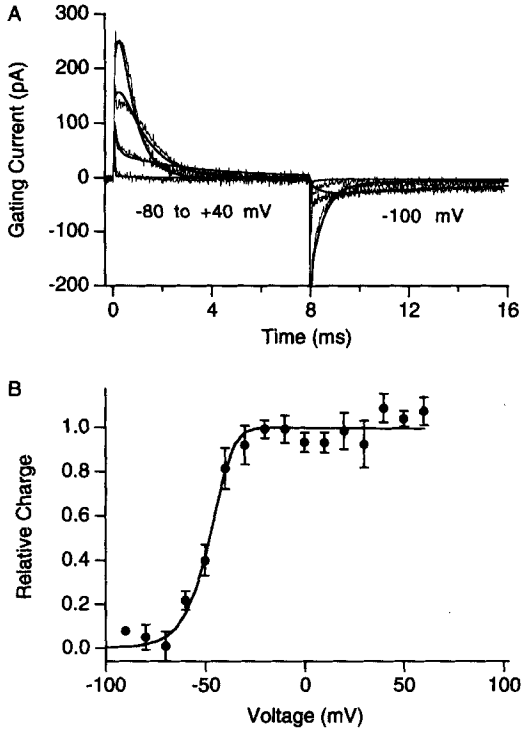

FIGURE 12. (*A*) The experimentally observed gating currents and the predictions of the model in Fig. 7 (*smooth curve*). The gating currents were elicited in response to voltage steps to −80 mV to +40 mV in increments of 40 mV from the holding voltage of −100 mV. The gating currents were measured as described in the previous paper (Zagotta et al., 1994). The leak holding voltage was +50 mV. The data were filtered at 8 kHz and digitized every 16 μs. The model parameters are described in Table I except that the closing rate was slowed by a factor of 4 by setting θ = 43. (*B*) Voltage dependence of the integrated ON charge movements. The smooth line represent the prediction of the model shown in Fig. 7. The ON gating currents during 16 ms pulses were integrated and normalized to the charge movement at depolarized voltages.

which will be markedly reduced due to filtering and has been cut off in Figs. 12 *A* and 14. Fig. 14 shows that both the data and the model exhibit larger and faster OFF gating currents following only 1 ms pulses to +50 mV. Once again, these OFF gating currents arise from channels that have not yet opened, and their time course is quite well described by the model. As discussed above, the time course of the OFF gating currents for channels that have not yet opened is significantly slower than expected for models in the classes A, B, or C. The class D model in Fig. 7 is able to produce these slow OFF gating currents by allowing the gating charge in each subunit to become locked in by the second transition in each subunit. Therefore, the reverse rate for the second transition becomes rate limiting for the return of the gating

charge for channels that have not yet opened. Furthermore, once the channel opens, the gating charge becomes further slowed by the slow first closing transition.

Reactivation. The rate of channel reactivation was measured by first applying a depolarizing pulse to open the channels, then a brief hyperpolarizing pulse to close a

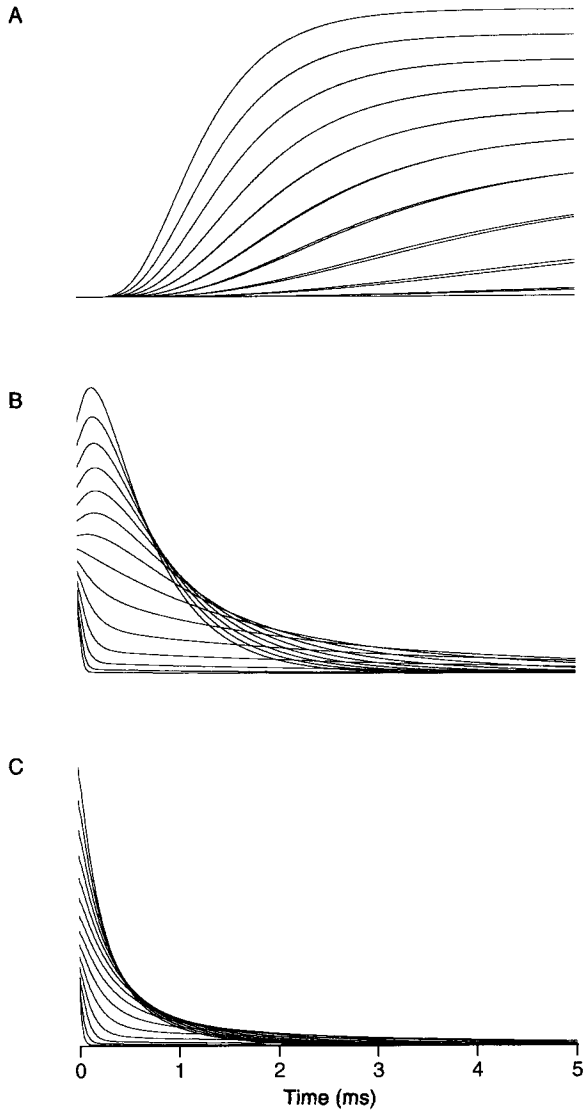

FIGURE 13. (*A*) Time course of the activation predicted by the model shown in Fig. 7. The currents were simulated in response to voltage pulses to −50 to +50 mV in increments of 10 mV. The probability of the channel being in C_1 was set to 1 at time $t = 0$. At each voltage, two sweeps were shown. One sweep was simulated with the slower rate corresponding to the first transition in each subunit as described in Table I and the other sweep was simulated using the slower rate corresponding to the second transition (α and γ values were reversed). (*B*) ON gating currents simulated in response to voltage pulses to −80 to +40 mV. The currents were simulated assuming that the first of the two transitions in the model shown in Fig. 7 is the slowest as described in Table I. (*C*) ON gating currents simulated in response to voltage pulses to −80 to +40 mV. The model parameters were as in Table I except that α and γ values were reversed.

fraction of the channels, and finally a second depolarizing pulse to reopen the closed channels. The reactivation time course represents a sensitive probe of the gating kinetics. To fit the reactivation data, a model must predict the distribution of channels among the closed states at each moment during the deactivation process at

hyperpolarized voltages, and predict the time course of opening from each of these initial distributions at depolarized voltages. Fig. 15 *A* shows the fits of the model in Fig. 7 to the reactivation time course after hyperpolarizing pulses to −70 mV of different duration. For these fits the predicted currents for each voltage step were scaled to account for the change in the driving force. Because the tail currents for this particular experiment were somewhat slower and the activation kinetics somewhat faster than the average behavior used to estimate the rate constants in the model of Fig. 7, the values of some of the rate constants were adjusted somewhat for these fits,

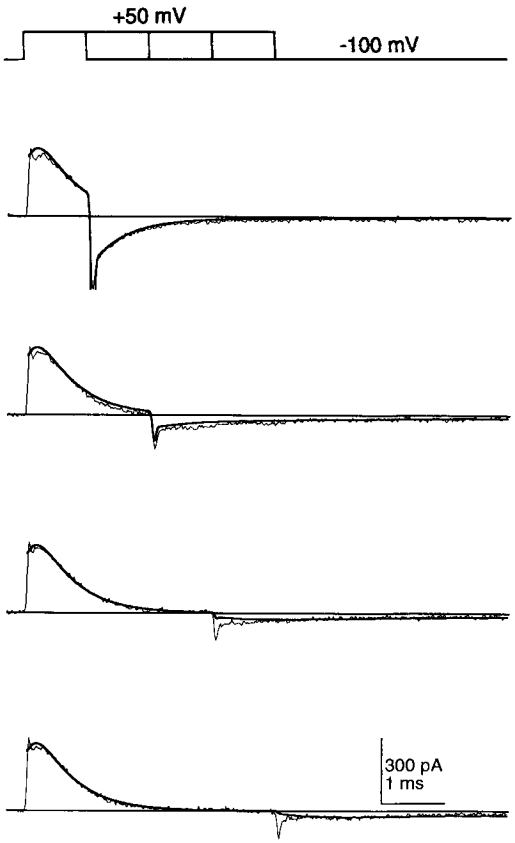

FIGURE 14. Observed and simulated OFF gating currents following voltage pulses to +50 mV for 1, 2, 3, and 4 ms from the holding voltage of −100 mV. The simulated gating currents are shown using the bold line. The gating currents were recorded as described in the previous paper (Zagotta et al., 1994). The data were filtered at 8 kHz and digitized every 18 μs. The gating currents were simulated using the parameters in Table I except that the closing rate was slowed by a factor of 4 by setting $\theta = 43$.

as described in the figure legend. After very short hyperpolarizing pulses to −70 mV, both the data and the model undergo rapid reactivation. In the model, this reactivation is occurring from two different pathways. Most channels reactivate from the state labeled C_{13} in Fig. 7, requiring a single subunit to undergo two conformational changes. A smaller fraction of channels reactivate from the C_f state. With longer hyperpolarizing pulses, the reactivation time course of both the data and the model becomes appreciably sigmoidal. Furthermore, the sigmoidal character is occurring well before deactivation is complete. This is shown for the model in Fig.

15 *B* by shifting the reactivation curves along the time axis to equate the final phases of their activation time courses. The sigmoidal character seen after moderate hyperpolarizations reflects a first closing transition that is slower than expected for independent subunits and is directly comparable to that seen in the data (Fig. 16 *B* of

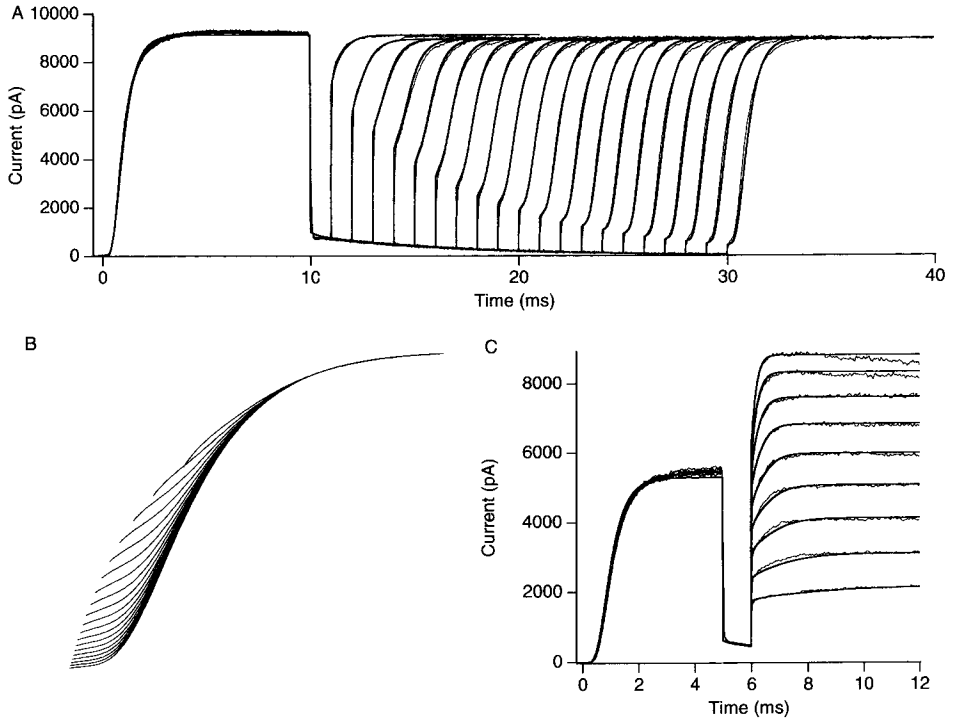

FIGURE 15. (*A*) Comparison of the observed and simulated ionic current reactivation time course. The currents were elicited in response to voltage pulses to +50 mV for 10 ms, then to −70 mV for different durations (1 to 20 ms) and back to +50 mV. The data were filtered at 4 kHz and digitized every 20 μs. The currents were simulated using the parameters described in Table I except that α = 1,261, β = 420, γ = 4,000, and θ = 10.9. This adjustment was necessary as the particular tail shown is slower than the average tail currents. The simulated data were scaled to account for the driving force. The probability of the channel being in C_1 was set to 1 at time t = 0. (*B*) Comparison of the sigmoidal characteristics of the currents during the reactivation. The currents were simulated as in *A*. The currents simulated during the second depolarizing pulse to +50 mV following hyperpolarizing pulses to −70 mV were shifted along the time axis to match the latter phase of the reactivation. (*C*) Voltage dependence of the reactivation. The currents were elicited in response to voltage pulses to +50 mV for 5 ms, then to −65 mV for 1 ms and to −20 to +140 mV in increments of 20 mV. The currents were filtered at 10 kHz and digitized every 10 μs. The currents were simulated using the parameters described in Table I except that α = 1,361 s^{-1} and β = 453 s^{-1}.

the previous paper [Zagotta et al., 1994]). The voltage dependence of the reactivation time course after short hyperpolarizing pulses was examined by varying the voltage of the second depolarizing pulse. Fig. 15 C shows that the model faithfully reproduces the reactivation time course between −20 and +140 mV.

Effect of holding voltage on the time course of reactivation. The model was also tested for its ability to predict the effect of holding voltage on the time course of activation. This experiment, originally done by Cole and Moore (Cole and Moore, 1960) for squid potassium channels, probes the equilibrium distribution of the channels among the closed states at different voltages. Fig. 16 *A* shows the model's predictions of the macroscopic activation time course for voltage steps to 0 mV from holding voltages between −125 and −45 mV. Like the experimental data shown in Fig. 5 *B* of the

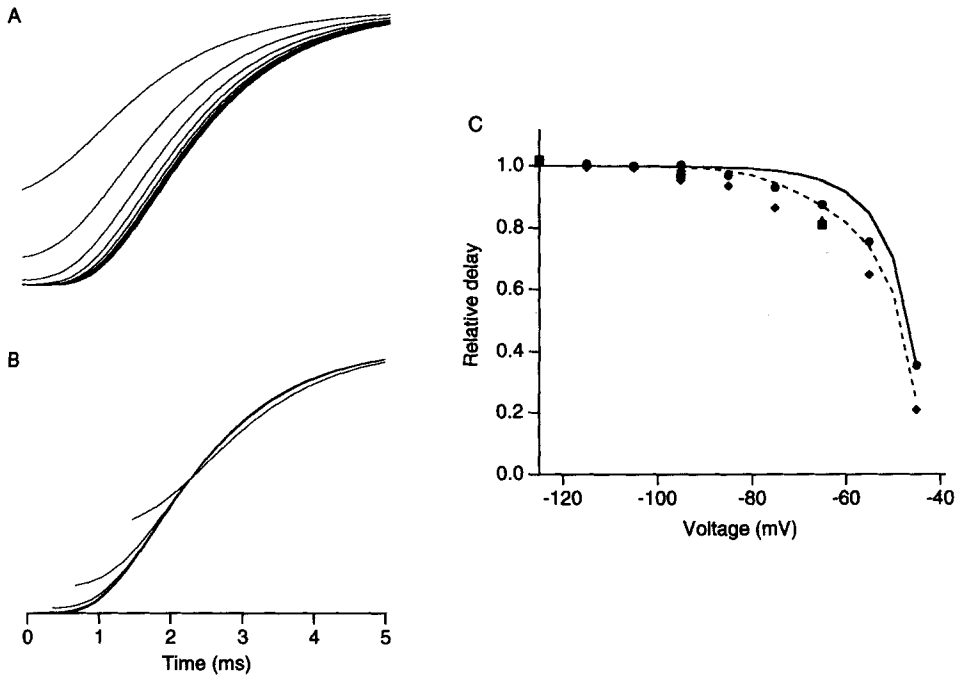

FIGURE 16. (*A*) The activation time course at 0 mV predicted by the model shown in Fig. 7 with different holding voltages (−100 to −40 mV in increments of 10 mV). From left to right, the data were simulated with a holding voltage of −40 to −100 mV. The time courses were simulated using the parameters described in Table I. (*B*) The simulated currents shown in *A* are shifted along the time axis relative to the record simulated with the holding voltage of −100 so that the half maximal amplitude times coincide. The delay time is defined as the time required for the superimposition. (*C*) The relative delay time as defined in *A* as a function of the holding voltage. Delay time measured with different holding voltages were normalized. The continuous line shows the prediction of the model shown in Fig. 7. The dashed line shows the prediction of the model shown in Fig. 17.

previous paper (Zagotta et al., 1994), the more depolarized holding voltages cause a decrease in the delay associated with the activation process. This decrease in delay arises because, at more depolarized holding voltages, many of the channels reside in closed states along the activation pathway nearer to the open state and therefore require fewer conformational transitions before opening. In Fig. 16 *B* the activation time course is shifted along the time axis so that the times to half maximal current coincide. Like the experimental data shown in Fig. 5 *C* of the previous paper

(Zagotta et al., 1994), the activation time courses overlay nearly perfectly with holding potentials below −50 mV, but are somewhat slower with more depolarized holding potentials.

The voltage dependence of the decreased delay, however, is different between the data and the model. Fig. 16 *C* plots the delay to half maximal current, normalized to the delay at −125 mV, as a function of holding voltage from several different patches and from the model in Fig. 7 (*solid line*). Clearly the data begins to develop a decrease in the delay at much more hyperpolarized voltages than the model. This suggests that, at these hyperpolarized voltages, the channels are distributed in closed states much nearer to the open state than the model predicts. This behavior might suggest some form of non-independent gating between the subunits beyond just a slow first closing transition. In fact model features that appear as a form of cooperativity, such as a concerted final transition or a slow first closing transition, cause the equilibrium distribution of the channels to be even more biased away from the open state at hyperpolarized voltages. For example, the cooperative model in Scheme III becomes more like a simple two state model between C_1 and O as the cooperativity factor ϕ is increased above 1.

The discussion above suggests that the voltage dependence of the Cole-Moore shift might be produced by a model like Scheme III where the cooperativity factor ϕ is decreased below 1, a form of negative cooperativity. A possible physical basis for such a scheme would be if the charge movement associated with the voltage-dependent conformational transitions in one subunit electrostatically inhibited the charge movement in other subunits. If all of the subunits influenced each other equally, than the equilibrium constant for each transition would be decreased by a constant cooperativity factor for each subunit that has already changed conformation, similar to Scheme III for a class A model. Furthermore, if the interactions do not influence the amount of charge movement before and after the transition state, then the kinetic rate constants would be affected in proportion to the amount of charge movement that they produce. Because the rates of the reverse transitions, in general, have a higher degree of voltage-dependence than those of forward transitions, the largest effect of this negative cooperativity will be on the reverse transitions.

For the class D models, involving two voltage-dependent conformation changes per subunit, we might expect that this electrostatic interaction between subunits might extend to the conformational changes occurring within a single subunit. Fig. 17 shows one way of implementing this type of mechanism into the model of Fig. 7. In this model each conformational transition that occurs has been proposed to exert an electrostatic effect on all subsequent transitions in proportion to the total amount of charge moved. Therefore the first transition in each subunit will slow the second transition in that subunit as well as the first and second transition of other subunits. The definitions of the variables in Fig. 17 are shown in the appendix. This modification of the model in Fig. 7 introduces one additional free parameter, η, that represents the voltage shift produced per unit gating charge already moved.

This model, with different values of η, was fitted to the voltage dependence of the steady state P_0 and to the macroscopic activation and deactivation time courses at different voltages. Because this model contains many free parameters that could not be determined independently, no attempt was made to optimize these fits. The

predictions of the model in Fig. 17 with $\eta = 2$ mV/e$^-$ for the voltage dependence of the Cole-Moore shift are shown superimposed on the data in Fig. 16 *C* (*dashed line*). Rates used for this fit are presented in Table II. While not producing a perfect fit, this model with an electrostatic interaction equivalent to 2 mV per electronic charge goes a long way in explaining the voltage dependence of the Cole-Moore shift. The value of η is quite small suggesting that these electrostatic interactions may indeed be significant. Other models for negative cooperativity might also account for these data.

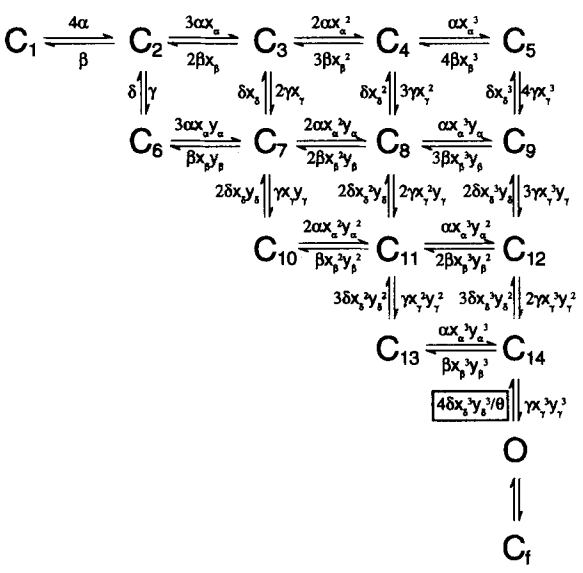

FIGURE 17. An extended class D model based on that shown in Fig. 7. This model incorporates electrostatic interaction between different subunits and the two conformational changes occurring within a single subunit. x_α, x_β, x_γ and x_δ indicate how much the values of α, β, γ, and δ are affected by the electrostatic effects induced by the first transition charge movements. y_α, y_β, y_γ, and y_δ indicate how much the values of α, β, γ, and δ are affected by the electrostatic effects induced by the second transition charge movements. x's and y's are functions of η, which represent the equivalent surface potential produced per unit charge already moved (see Appendix).

DISCUSSION

In this paper we have considered a number of gating models to account for the steady state and kinetic phenomena discussed in the previous two papers (Hoshi et al., 1994; Zagotta et al., 1994). We have shown that virtually all of this steady state and kinetic behavior can be produced by a class D model where the opening of the channel requires two conformational changes in each of four subunits. The gating in each subunit was considered to be independent except for a slow first closing transition and a short-lived closed state C_f that occurs after opening. From the rate constants, the free energy differences between the various states (ΔG) can be calculated with the following equation:

$$\Delta G = -RT \ln\left(\frac{k_1}{k_{-1}}\right) \tag{5}$$

where k_1 is the rate of the forward reaction and k_{-1} is the rate of the reverse reaction.

This free energy difference indicates the relative stability of the different channel conformations represented by different states. At 0 mV the activated conformation of each subunit is 2.9 kcals/mol more stable than the middle resting conformation R2 and 3.5 kcals/mol more stable than the left resting conformation R1, producing a high steady state open probability. Furthermore, to account for the slowing of the first closing transition, there is an additional increase in stability of 1.3 kcals/mole when the channel enters the open state: this extra stability could arise from a number of factors. (*a*) Interactions between the subunits, such as cooperative interactions could produce an added stability when all of the subunits are in their activated conformation. (*b*) The open state could be more heavily hydrated than the closed states as has been proposed from the effects of solvent on the open probability and activation time course of both sodium and potassium channels (Alicata, Rayner, and Starkus, 1989, 1990; Rayner, Starkus, Ruben, and Alicata, 1992; Schauf and Bullock, 1979, 1980, 1982; Zimmerberg, Bezanilla, and Parsegian, 1990). (*c*) The channel might close more slowly when ions are in the pore; a mechanism that has been called the occupancy hypothesis (Ascher, Marty, and Neild, 1978; Marchais and Marty,

TABLE II

Summary of the Rate Constants for the Model in Fig. 17

Rate constant	k_o	z_k
k	s^{-1}	e^- *charges*
α	1010	0.32
β	6.25	2.5
γ	3400	0.32
δ	8.5	1.1
$O \rightarrow Cf$	600	0
$Cf \rightarrow O$	3800	0.17

The variables are defined in the Appendix. The value of θ is 11.8, and the value of η is 2 mV/e^- charge.

1979; Matteson and Swenson, 1986; Swenson and Armstrong, 1981). This mechanism has been proposed to account for the slowing of deactivation in various voltage-dependent potassium channels due to certain external monovalent cations (Cahalan, Chandy, DeCoursey, and Gupta, 1985; Matteson and Swenson, 1986; Sala and Matteson, 1991; Shapiro and DeCoursey, 1991*a*, *b*; Spruce, Standen, and Stanfield, 1989; Swenson and Armstrong, 1981), an effect demonstrated for Rb^+ on *Shaker* channels in Fig. 13 of the previous paper (Zagotta et al., 1994).

The model exhibits a number of features of gating described in the previous papers (Hoshi et al., 1994; Zagotta et al., 1994), including: (*a*) a total gating charge, equivalent to 13 electronic charges moving through the membrane electric field; (*b*) the requirement for at least five or six transitions before opening from hyperpolarized voltages (the model requires eight transitions); (*c*) a similar amount of voltage-dependence in all of the forward kinetic transitions (the equivalent of 0.25 or 0.32 charges moving before the transition states; (*d*) considerably more charge movement after the transition states (the equivalent of 1.6 or 1.1 charges) than before the transition states; (*e*) a first closing transition that is slower than expected for

independent and identical transitions; (*f*) a short-lived closed state not in the activation pathway.

This class D model can quantitatively account for a number of steady state and kinetic measurements, including: (*a*) the voltage-dependence of the steady state probability of being open as measured from both the pulse and tail currents; (*b*) the macroscopic activation time course between −50 and +50 mV and the deactivation time course between −40 and −120 mV; (*c*) the dependence of reactivation on the duration of the hyperpolarizing pulse; (*d*) the single channel first latencies, open times, and rapid component of the closed times between −40 and 50 mV and the voltage-dependence of the open times between −90 and −50 mV; (*e*) the voltage-dependence of the steady state charge movement; (*f*) the time course of the ON gating currents between −60 and +50 mV (including a small rising phase above −20 mV) and of the OFF gating currents at −100 mV; (*g*) the dependence of the time course of the OFF gating currents on the duration and amplitude of the depolarizing pulse.

A few other properties of the channel are poorly described by the model in its current form. Many of these shortcomings, however, can be alleviated by introducing additional features to the model. The model adequately describes the general behavior of the tail currents and OFF gating current kinetics. However the predictions differ quantitatively from the time courses of these measurements. The experimental tail currents exhibit a multiexponential time course that is not predicted by the model of Fig. 7. As discussed previously, this at least in part, comes from the C_i state that is not included in the model. The decay of the OFF gating currents slows with longer duration voltage pulses. However, the OFF gating currents from the experiments in Figs. 12 and 14 show a rapidly decaying component with long pulses to depolarized voltage that is not predicted by the model. In our experiments, the kinetics of these OFF gating currents were highly variable with different experimental conditions and subtraction protocols. Because of this, we are less confident in the model's predictions for the OFF gating currents than we are in other predictions of the model. However, the model can readily account for the range of OFF gating current kinetics by varying the amount of slowing of the first closing transition.

As shown in Fig. 16, the model predicts that the effect of holding voltage on the time course of activation is saturated below −80 mV, while experimentally, the sigmoidal delay continues to increase with holding potentials down to −100 mV. This discrepancy was largely alleviated by introducing a negative cooperativity in the activation process. The negative cooperativity was proposed to arise from electrostatic repulsion of the gating charge from each subunit. This mechanism will only affect the rate of the voltage-dependent transitions, and therefore will have a greater influence on the reverse transitions. The model also predicts a somewhat faster decay in the ON gating currents with steps to between −80 and −60 mV. This problem is also largely alleviated by the addition of negative cooperativity (data not shown). A small amount of negative cooperativity causes a slight decrease in the slope of the steady state P_0 vs voltage relation at high Po and therefore requires somewhat more charge movement to fit this relation. However, because this mechanism of negative

cooperativity introduces an additional free parameter and is probably not the only way of reproducing the effects described here, it was not developed further.

The model shown in Fig. 7 also does not exhibit the intermediate component in the distribution of closed durations at depolarized voltages that was described in the first paper (Hoshi et al., 1994). As indicated in the first paper, the closed state(s) that contribute to these intermediate closed durations, designated C_i, cannot always be traversed in the process of opening, and therefore we consider them not to be part of the normal activation process. Transitions to the Ci state may occur from the open state and/or the C_f state and may also occur as a branch from one or more of the closed states in the activation pathway. Note that if the C_i state can only be entered from the open or C_f states, it will appear as a nonabsorbing inactivated state and cause a small ($\sim$10%) decline in the peak current. Because of the relatively slow kinetics associated with the Ci state and of uncertainty in its coupling to the other states, it has not been explicitly included in the model of Fig. 7.

N-type inactivation has been proposed to occur by a ball and chain mechanism whereby the amino terminal domain blocks the channel (Hoshi et al., 1990; Zagotta et al., 1990). Since this model was formulated for ShBΔ6-46 channels, it does not contain an *N*-type inactivated state. We have shown previously that *N*-type inactivation, when present, is coupled to the activation process (Zagotta and Aldrich, 1990*b*; Zagotta, Hoshi, and Aldrich, 1989). Furthermore, the increase in open durations when *N*-type inactivation is disrupted indicates that the channel can directly inactivate from the open state (Hoshi et al., 1990). However the coupling is not complete and the channel can occasionally undergo inactivation before opening as indicated by the occurrence of relatively long voltage pulses without openings (Zagotta and Aldrich, 1990*b*). This suggests that the *N*-type inactivated state can be entered from both the open state and some of the closed states in the activation pathway. One possible scenario is if *N*-type inactivation can only occur if all four subunits have undergone the first conformational transition, producing a transition to an *N*-type inactivated state from each of the closed states on the right side of the expanded model in Fig. 7.

While the *N*-type inactivation process in these channels has been effectively removed by the deletion of amino acids 6-46, these channels are still able to under a second type of inactivation process referred to as C-type inactivation (Hoshi et al., 1991). Like *N*-type inactivation, *C*-type inactivation occurs with a rate that is not appreciably voltage dependent at depolarized voltages and is therefore thought to be coupled to activation. However, *C*-type inactivation is quite slow compared to the time scale of the experiments presented here and was therefore not explicitly included in the model of Fig. 7.

As in all kinetic analyses, our ability to identify discrete states is limited by the bandwidth of our recordings. States with very rapid kinetics would not be detected. For example, a final open-closed transition that is very fast would appear, at limited bandwidth, as simply a reduction in the single-channel current. In some cases, the apparent rate constant for a transition will be influenced by these rapid states. For example, if the channel cannot close with an ion in the pore, as proposed in the occupancy hypothesis, then the apparent rate constant for the closing transition will represent the product of the true closing rate constant and the probability that the

channel is not occupied. The occupied and unoccupied open states will appear kinetically as one state because the rate of ions entering and leaving the pore is very rapid. Therefore, the slow apparent closing transition may not be due to an intrinsically slow conformational change but, instead due to a state with rapid kinetics that cannot close.

In this paper we have also considered a number of other kinetic models to describe the voltage-dependent activation process. We have restricted our analysis to models that involve four identical, though not necessarily independent, processes so that the models could be interpreted in terms of conformational changes in individual subunits and concerted conformational changes. We have also assumed that the voltage-dependent rate constants are exponentially dependent on voltages as expected for a simple movement of charge or reorientation of a dipole in the membrane electric field. While other more complex forms of voltage-dependencies are possible (Stevens, 1978), these would introduce additional free parameters causing the models to be poorly constrained. Given these constraints, three commonly considered classes of models were found not to describe the data adequately: (*a*) class A models, with and without cooperativity, involving only one conformational change in each of four subunits before opening; (*b*) class B models, involving a conformational change in each subunit followed by a concerted conformational change; (*c*) and class C models, involving a concerted conformational change that is promoted by a conformational change in each subunit. Class D and E models, which can reproduce virtually all of our results, require two conformational changes in each subunit and differ only in whether the two transitions are absolutely coupled (class D) or partially coupled (class E).

Many models similar to those shown in Fig. 1 have been considered by other investigators to describe the activation of voltage-dependent potassium channels from different sources. However, none of these previous models can account for all of the observations reported for the *Shaker* channel in the previous paper (Zagotta et al., 1994), especially those involving the sigmoidal delay and its voltage dependence. The model of Hodgkin and Huxley (1952) for the squid voltage-dependent potassium channel is a class A model with four independent and identical transitions. As discussed in detail in the previous paper (Zagotta et al., 1994), the gating behavior departs in many ways from the predictions of independent and identical transitions. In addition, four transitions cannot account for the observed sigmoidal delay, even if the independence constraint is relaxed. The model of Cole and Moore (Cole and Moore, 1960), while producing plenty of sigmoidal delay, is still based on independent and identical gating particles and is not easily interpreted in terms of the conformational changes in four subunits. The slow transitions in the models of Gilly and Armstrong (1982) and White and Bezanilla (1985) would reduce the sigmoidal delay of these schemes with six transitions to below that seen in the *Shaker* channel. Zagotta and Aldrich (1990*b*) proposed a class B model for *Shaker* channels with four independent and identical transitions followed by a final, voltage-independent concerted transition. Once again, this model would not produce nearly enough sigmoidal delay, particularly at depolarized voltages where the voltage-independent transition would be rate limiting. In addition the deactivation time course would be voltage-independent and slow below −80 mV. Koren et al. (1990) proposed a similar

model for the RCK1 channels but with a considerably faster voltage-independent transition that would not become rate limiting for activation or deactivation in the voltage-range tested. However, a fast final opening transition will be kinetically transparent at depolarized voltages and would not be adequate to produce the sigmoidal delay seen in *Shaker* channels. The addition of cooperativity to this scheme, as proposed by Tytgat and Hess (1992), will reduce the delay even further. A class C model, with a voltage-independent concerted opening transition that is not absolutely coupled to the voltage-dependent transitions, was proposed for voltage-dependent calcium channels and recently extended to potassium channels (Greene and Jones, 1993; Marks and Jones, 1992). Unlike the model of Zagotta and Aldrich (1990*b*), this model will produce a voltage-dependent deactivation rate as observed. However, at depolarized voltages it will still exhibit a sigmoidal delay that is too small and decreases with increasing depolarization. A class D model was proposed to account for the effect of holding potential on the activation time course of crayfish potassium channels (Young and Moore, 1981), but was not developed quantitatively. In addition Keynes has proposed a class D model for the activation gating of the squid sodium channel (Keynes, 1991; Keynes, Greeff, and Forster, 1990).

The values of the parameters in the model of Fig. 7 are expected to vary considerably among different types of voltage-dependent potassium channels. Small quantitative differences in the energies for the states and transition states can cause quite large differences in the rates of the transitions and the macroscopic kinetic behavior. In addition, the form of the model may not be applicable to some potassium channels. The assumption of four identical processes occurring during activation may not be valid for some other channel types. While the voltage-dependent sodium and calcium channels contain four homologous domains, small differences in sequence may cause these domains to have very different gating behavior. This is exemplified in voltage-dependent calcium channels (Tanabe, Adams, Numa, and Beam, 1991) where a kinetic study of chimeric channels between skeletal muscle and cardiac calcium channels has indicated that the activation time course is dominated by the gating in the first domain.

Most ligand-gated channels are heteromultimeric and contain binding domains in only some of their subunits. For example the acetylcholine-activated channel contains only two Ach binding sites. The gating of this channel has frequently been modeled as a two binding reactions followed by a concerted conformational change, similar to a class B model with only two activatable subunits (Sine, Claudio, and Sigworth, 1990). Interestingly, it has recently been shown that a model requiring Ach binding and a subsequent conformation change in each of two subunits before opening produced a significantly better fit to the single-channel data (Auerbach, 1993). This model is similar to the class D models considered here where the first transition in each subunit is simply the binding of ligand. Furthermore a significantly better fit was produced if the first closing transition was slower than expected for independent subunits, as occurs in the model of Fig. 7.

The model in Fig. 7 can account for some of the observed alterations in gating better than a model based on the Hodgkin and Huxley (1952) formulation. Many mutations have been found in the S4 segment, the S4-S5 linker, and the S5 segment that profoundly alter the voltage-dependent activation process (Gautam and

Tanouye, 1990; Lichtinghagen, Stocker, Wittka, Boheim, Stuhmer, Ferrus, and Pongs, 1990; Liman et al., 1991; Lopez, Jan, and Jan, 1991; McCormack, Tanouye, Iverson, Lin, Ramaswami, McCormack, Campanelli, Mathew, and Rudy, 1991; Papazian, Timpe, Jan, and Jan, 1991; Schoppa et al., 1992; Stuhmer, Conti, Suzuki, Wang, Noda, Yahagi, Kubo, and Numa, 1989; Zagotta and Aldrich, 1990*a*). In several cases an apparent decrease in the slope of the steady state P_0 vs voltage relation occurred with mutations that preserved the charge on the mutated residue or altered uncharged residues (Gautam and Tanouye, 1990; Lopez et al., 1991; McCormack et al., 1991; Papazian et al., 1991; Schoppa et al., 1992; Zagotta and Aldrich, 1990*a*). In other cases the apparent decrease in slope due to a mutation was larger than expected even if the mutated residue moved though the entire membrane electric field (Liman et al., 1991). These results are hard to reconcile with a model containing a single voltage-dependent conformational change per subunit. However a model containing multiple types of voltage-dependent transitions can account for these results with a differential effect of the mutation on the different transitions. A second type of voltage-dependent transition was suggested by Schoppa et al. (1992) to account for the apparent decrease in slope of the steady state P_0 vs voltage relation due to a mutation of a leucine residue in the S4 segment. They also showed that the mutation separated the gating current into two components consistent with two types of voltage-dependent conformational changes that occur in different voltage ranges in the mutant channels. The additional voltage-dependent transitions could arise from either multiple conformational changes per subunit or from multiple concerted conformational changes.

The slow first closing transition in the model of Fig. 7 might also account for some of the observed alterations in gating. For channels that have reached the open state, the OFF gating currents have ranged from very slow, low amplitude currents to transient, moderate amplitude currents with a clearly discernible rising phase (Bezanilla, Perozo, Papazian, and Stefani, 1991; Schoppa et al., 1992; Stuhmer et al., 1991). This range of behavior can be reproduced by varying only the rate of the first closing transition.

The interactions between subunits have been explored by examining some S4 mutations in heteromultimeric channels, containing the mutation in only some of their subunits (Hurst, Kavanaugh, Yakel, Adelman, and North, 1992; Tytgat and Hess, 1992). The steady state voltage dependence of the activation process in these heteromultimers was not as expected for independent subunits, but, instead, was consistent with cooperative interactions between subunits. Tytgat and Hess (1992) modeled these cooperative interactions as a constant energy of stabilization for the activation conformation of a subunit when a neighboring subunit is activated. However a model with a slow first closing transition can quantitatively account for the voltage-dependence of activation in heteromultimers with no other cooperative interactions. In addition, the rising phase of the ON gating currents is frequently taken as evidence for cooperative interactions between the subunits during activation. However, the model in Fig. 7 would produce a rising phase even if the subunits were completely independent. In fact the addition of cooperativity generally produces a poor fit to the voltage-dependence of the Cole-Moore shift. For this reason we have

introduced a negative cooperativity in the model of Fig. 17 to account for these Cole-Moore data (as shown in Fig. 16).

APPENDIX

The models in Fig. 7 and 16 both consider that the opening of the channel requires two voltage-dependent conformational changes in each of four identical subunits. The transitions in each subunit can be summarized by the following scheme:

$$R_1 \underset{\beta}{\overset{\alpha}{\rightleftharpoons}} R_2 \underset{\delta}{\overset{\gamma}{\rightleftharpoons}} A$$

SCHEME IX

The rate constants were assumed to be exponentially dependent on voltage, and are given by the following expression:

$$\alpha = \alpha_0 e^{z_\alpha FV/RT} \tag{A1}$$

$$\beta = \beta_0 e^{-z_\beta FV/RT} \tag{A2}$$

$$\gamma = \gamma_0 e^{z_\gamma FV/RT} \tag{A3}$$

$$\delta = \delta_0 e^{-z_\delta FV/RT} \tag{A4}$$

where α_0, β_0, γ_0, and δ_0 are the values of the rate constants at 0 mV; $z_\alpha z_\beta$, z_γ, and z_δ are the equivalent charge movements up to the transition state for each transition; F is Faraday's constant, R is the universal gas constant; and T is the absolute temperature. The total charge moved for the first transition in each subunit is given by the following expression:

$$z_x = z_\alpha + z_\beta \tag{A5}$$

and the total charge moved for the second transition in each subunit is given by the following expression:

$$z_y = z_\gamma + z_\delta. \tag{A6}$$

Because all of the subunits are considered to be identical, the charge movement associated with the transitions in different subunits is assumed to be unaltered by the nonindependent gating and cooperative interactions discussed below.

For the model in Fig. 7, the gating of the different subunits is considered to be independent except for the C_f state and a slower first closing transition. The first closing transition is slowed by the factor θ. This produces a model that contains nine free parameters for the transitions before first opening: α_0, β_0, γ_0, δ_0, z_α, z_β, z_γ, z_δ, and θ. In addition, the model contains three free parameters for the transitions after opening, the $O \rightarrow C_f$ rate, the $C_f \rightarrow O$ rate, and the voltage dependence of the $C_f \rightarrow O$ rate (the $O \rightarrow C_f$ rate was considered to be voltage-independent).

For the model in Fig. 17, interactions between subunits have been assumed to occur by an electrostatic mechanism. In this model each voltage-dependent conformational transition that occurs exerts an electrostatic effect on all subsequent voltage-dependent transitions. This electrostatic mechanism has been introduced by

assuming a constant voltage offset per unit of gating charge moved (η) as would be expected if the gating charge behaved like surface charge for all subsequent transitions. The effect of these electrostatic interactions will be to decrease the rate of forward transitions and to increase the rate of reverse transitions as the channel approaches the open state, a form of negative cooperativity. However, because the reverse transitions are considerably more voltage dependent than the forward transitions, they will be disproportionally affected. The factor by which each rate is affected is shown in Fig. 17, where the x's and y's are given by the following expressions:

$$x_\alpha = e^{-z_\alpha z_x \eta F/RT} \tag{A7}$$

$$x_\beta = e^{z_\beta z_x \eta F/RT} \tag{A8}$$

$$x_\gamma = e^{-z_\gamma z_x \eta F/RT} \tag{A9}$$

$$x_\delta = e^{z_\delta z_x \eta F/RT} \tag{A10}$$

$$y_\alpha = e^{-z_\alpha z_y \eta F/RT} \tag{A11}$$

$$y_\beta = e^{z_\beta z_y \eta F/RT} \tag{A12}$$

$$y_\gamma = e^{-z_\gamma z_y \eta F/RT} \tag{A13}$$

$$y_\delta = e^{z_\delta z_y \eta F/RT} \tag{A14}$$

The rate constants α, β, γ, and δ are defined as the transition rates in each subunit when the other three subunits are in the R_1 state. This mechanism for subunit interactions introduces one additional free parameter (η) to the modeling.

We thank Tom Middendorf and Max Kanevsky for helpful comments on the manuscript and Jeremy Dittman for collaboration on some of the gating current experiments.

This work was supported by a grant from National Institutes of Health (NS23294) and by a National Institute of Mental Health Silvio Conte Center for Neuroscience Research Grant (MH 48108). W. N. Zagotta is a Warner-Lambert fellow of the Life Sciences Research Foundation. R. W. Aldrich is an investigator with the Howard Hughes Medical Institute.

Original version received 13 May 1993 and accepted version received 27 August 1993.

REFERENCES

Alicata, D. A., M. D. Rayner, and J. G. Starkus. 1989. Osmotic and pharmacological effects of formamide on capacity current, gating current, and sodium current in crayfish giant axons. *Biophysical Journal.* 55:347–353.

Alicata, D. A., M. D. Rayner, and J. G. Starkus. 1990. Sodium channel activation mechanisms. Insights from deuterium oxide substitution. *Biophysical Journal.* 57:745–758.

Almers, W. 1978. Gating currents and charge movements in excitable membranes. *Review of Physiology and Biochemical Pharmacology.* 82:96–190.

Andersen, O. S., and R. E. Koeppe. 1992. Molecular determinants of channel function. *Physiological Reviews.* 72:S89–158.

Armstrong, C. M. 1981. Sodium channels and gating currents. *Physiological Reviews.* 61:644–683.

Armstrong, C. M., and F. Bezanilla. 1974. Charge movement associated with the opening and closing of the activation gates of the Na channels. *Journal of General Physiology.* 63:533–552.

Ascher, P., A. Marty, and T. O. Neild. 1978. Life time and elementary conductance of the channels mediating the excitatory effects of acetylcholine in Aplysia neurones. *Journal of Physiology.* 278:177–206.

Auerbach, A. 1993. A statistical analysis of acetylcholine receptor activation in *Xenopus* myocytes: stepwise *versus* concerted models of gating. *Journal of Physiology.* 461:339–378.

Bezanilla, F., E. Perozo, D. M. Papazian, and E. Stefani. 1991. Molecular basis of gating charge immobilization in *Shaker* potassium channels. *Science.* 254:679–683.

Blatz, A. L., and K. L. Magleby. 1986. Correcting single channel data for missed events. *Biophysical Journal.* 49:967–980.

Cahalan, M. D., K. G. Chandy, T. E. DeCoursey, and S. Gupta. 1985. A voltage-gated potassium channel in human T lymphocytes. *Journal of Physiology.* 358:197–237.

Cole, K. S., and J. W. Moore. 1960. Potassium ion current in the squid giant axon: dynamic characteristic. *Biophysical Journal.* 1:1–14.

Gautam, M., and M. A. Tanouye. 1990. Alteration of potassium channel gating: molecular analysis of the *Drosophila* Sh5 mutation. *Neuron.* 5:67–73.

Gilly, W. F., and C. M. Armstrong. 1982. Divalent cations and the activation kinetics of potassium channels in squid giant axons. *Journal of General Physiology.* 79:965–996.

Greene, K. J., and S. W. Jones. 1993. An allosteric model for the delayed rectifier potassium current of frog sympathetic neurons. *Biophysical Journal.* 64:312*a*. (Abstr.)

Hill, T. L., and Y. D. Chen. 1971*a*. On the theory of ion transport across the nerve membrane. 3. Potassium ion kinetics and cooperativity (with x = 4, 6, 9). *Proceedings of the National Academy of Sciences, USA.* 68:2488–2492.

Hill, T. L., and Y. D. Chen. 1971*b*. On the theory of ion transport across the nerve membrane. II. Potassium ion kinetics and cooperativity (with x = 4). *Proceedings of the National Academy of Sciences, USA.* 68:1711–1715.

Hodgkin, A. L., and A. F. Huxley. 1952. A quantitative description of membrane current and its application to conduction and excitation in nerve. *Journal of Physiology.* 117:500–544.

Hoshi, T., W. N. Zagotta, and R. W. Aldrich. 1990. Biophysical and molecular mechanisms of *Shaker* potassium channel inactivation. *Science.* 250:533–538.

Hoshi, T., W. N. Zagotta, and R. W. Aldrich. 1991. Two types of inactivation in *Shaker* K^+ channels: effects of alterations in the co-boxy-terminal region. *Neuron.* 7:547–556.

Hoshi, T., W. N. Zagotta, and R. W. Aldrich. 1994. *Shaker* potassium channel gating I: Transitions near the open state. *Journal of General Physiology.* 103:249–278.

Hurst, R. S., M. P. Kavanaugh, J. Yakel, J. P. Adelman, and R. A. North. 1992. Cooperative interactions among subunits of a voltage-dependent potassium channel. Evidence from expression of concatenated cDNAs. *Journal of Biological Chemistry.* 267:23742–23745.

Keynes, R. D. 1991. On the voltage dependence of inactivation in the sodium channel of the squid giant axon. *Proceedings of the Royal Society of London B.* 243:47–53.

Keynes, R. D., N. G. Greeff, and I. C. Forster. 1990. Kinetic analysis of the sodium gating current in the squid giant axon. *Proceedings of the Royal Society of London B.* 240:411–423.

Koren, G., E. R. Liman, D. E. Logothetis, G. B. Nadal, and P. Hess. 1990. Gating mechanism of a cloned potassium channel expressed in frog oocytes and mammalian cells. *Neuron.* 4:39–51.

Lichtinghagen, R., M. Stocker, R. Wittka, G. Boheim, W. Stuhmer, A. Ferrus, and O. Pongs. 1990. Molecular basis of altered excitability in Shaker mutants of *Drosophila* melanogaster. *EMBO Journal.* 9:4399–4407.

Liman, E. R., P. Hess, F. Weaver, and G. Koren. 1991. Voltage-sensing residues in the S4 region of a mammalian K+ channel. *Nature.* 353:752–756.

Lopez, G. A., Y. N. Jan, and L. Y. Jan. 1991. Hydrophobic substitution mutations in the S4 sequence alter voltage-dependent gating in *Shaker* K^+ channels. *Neuron.* 7:327–336.

MacKinnon, R. 1991. Determination of the subunit stoichiometry of a voltage-activated potassium channel. *Nature.* 350:232–235.

Marchais, D., and A. Marty. 1979. Interaction of permeant ions with channels activated by acetylcholine in Aplysia neurones. *Journal of Physiology.* 297:9–45.

Marks, T. N., and S. W. Jones. 1992. Calcium currents in the A7r5 smooth muscle-derived cell line. An allosteric model for calcium channel activation and dihydropyridine agonist action. *Journal of General Physiology.* 99:367–390.

Matteson, D. R., and R. J. Swenson. 1986. External monovalent cations that impede the closing of K channels. *Journal of General Physiology.* 87:795–816.

McCormack, K., M. A. Tanouye, L. E. Iverson, J. W. Lin, M. Ramaswami, T. McCormack, J. T. Campanelli, M. K. Mathew, and B. Rudy. 1991. A role for hydrophobic residues in the voltage-dependent gating of *Shaker* K^+ channels. *Proceedings of the National Academy of Sciences, USA.* 88:2931–2935.

McManus, O. B., and K. L. Magleby. 1989. Kinetic time constants independent of previous single-channel activity suggest Markov gating for a large conductance Ca-activated K channel. *Journal of General Physiology.* 94:1037–1070.

McManus, O. B., C. E. Spivak, A. L. Blatz, D. S. Weiss, and K. L. Magleby. 1989. Fractal models, Markov models, and channel kinetics. *Biophysical Journal.* 55:383–385.

Monod, J., J. Wyman, and J. P. Changeux. 1965. On the nature of allosteric transitions: a plausible model. *Journal of Molecular Biology.* 12:88–118.

Papazian, D. M., L. C. Timpe, Y. N. Jan, and L. Y. Jan. 1991. Alteration of voltage-dependence of *Shaker* potassium channel by mutations in the S4 sequence. *Nature.* 349:305–310.

Perozo, E., D. M. Papazian, E. Stefani, and F. Bezanilla. 1992. Gating currents in *Shaker* K^+ channels. Implications for activation and inactivation models. *Biophysical Journal.* 62:160–168–171.

Rayner, M. D., J. G. Starkus, P. C. Ruben, and D. A. Alicata. 1992. Voltage-sensitive and solvent-sensitive processes in ion channel gating. Kinetic effects of hyperosmolar media on activation and deactivation of sodium channels. *Biophysical Journal.* 61:96–108.

Sala, S., and D. R. Matteson. 1991. Voltage-dependent slowing of K channel closing kinetics by Rb+. *Journal of General Physiology.* 98:535–554.

Schauf, C. L., and J. O. Bullock. 1979. Modifications of sodium channel gating in Myxicola giant axons by deuterium oxide, temperature, and internal cations. *Biophysical Journal.* 27:193–208.

Schauf, C. L., and J. O. Bullock. 1980. Solvent substitution as a probe of channel gating in Myxicola. Differential effects of D20 on some components of membrane conductance. *Biophysical Journal.* 30:295–305.

Schauf, C. L., and J. O. Bullock. 1982. Solvent substitution as a probe of channel gating in Myxicola. Effects of D20 on kinetic properties of drugs that occlude channels. *Biophysical Journal.* 37:441–452.

Schoppa, N. E., K. McCormack, M. A. Tanouye, and F. J. Sigworth. 1991. High time-resolution recordings from oocytes injected with wild-type and V1 mutant *Shaker* 29-4 cDNAs. *Biophysical Journal.* 59:196*a*. (Abstr.)

Schoppa, N. E., K. McCormack, M. A. Tanouye, and F. J. Sigworth. 1992. The size of gating charge in wild-type and mutant *Shaker* potassium channels. *Science.* 255:1712–1715.

Shapiro, M. S., and T. E. DeCoursey. 1991*a*. Permeant ion effects on the gating kinetics of the type L potassium channel in mouse lymphocytes. *Journal of General Physiology.* 97:1251–1278.

Shapiro, M. S., and T. E. DeCoursey. 1991*b*. Selectivity and gating of the type L potassium channel in mouse lymphocytes. *Journal of General Physiology.* 97:1227–1250.

Sine, S. M., T. Claudio, and F. J. Sigworth. 1990. Activation of Torpedo acetylcholine receptors expressed in mouse fibroblasts. Single channel current kinetics reveal distinct agonist binding affinities. *Journal of General Physiology.* 96:395–437.

Spruce, A. E., N. B. Standen, and P. R. Stanfield. 1989. Rubidium ions and the gating of delayed rectifier potassium channels of frog skeletal muscle. *Journal of Physiology.* 411:597–610.

Stevens, C. F. 1978. Interactions between intrinsic membrane protein and electric field. An approach to studying nerve excitability. *Biophysical Journal.* 22:295–306.

Stuhmer, W., F. Conti, M. Stocker, O. Pongs, and S. H. Heinemann. 1991. Gating currents of inactivating and non-inactivating potassium channels expressed in *Xenopus* oocytes. *Pflügers Archiv.* 418:423–429.

Stuhmer, W., F. Conti, H. Suzuki, X. D. Wang, M. Noda, N. Yahagi, H. Kubo, and S. Numa. 1989. Structural parts involved in activation and inactivation of the sodium channel. *Nature.* 339:597–603.

Swenson, R. J., and C. M. Armstrong. 1981. K^+ channels close more slowly in the presence of external K^+ and Rb^+. *Nature.* 291:427–429.

Tanabe, T., B. A. Adams, S. Numa, and K. G. Beam. 1991. Repeat I of the dihydropyridine receptor is critical in determining calcium channel activation kinetics. *Nature.* 352:800–803.

Tytgat, J., and P. Hess. 1992. Evidence for cooperative interactions in potassium channel gating. *Nature.* 359:420–423.

Vandenberg, C. A., and F. Bezanilla. 1991. A sodium channel gating model based on single channel, macroscopic ionic, and gating currents in the squid giant axon. *Biophysical Journal.* 60:1511–1533.

White, M. M., and F. Bezanilla. 1985. Activation of squid axon K^+ channels. Ionic and gating current studies. *Journal of General Physiology.* 85:539–554.

Young, S. H., and J. W. Moore. 1981. Potassium ion currents in the crayfish giant axon. Dynamic characteristics. *Biophysical Journal.* 36:723–733.

Zagotta, W. N., and R. W. Aldrich. 1990a. Alterations in activation gating of single *Shaker* A-type potassium channels by the Sh5 mutation. *Journal of Neuroscience.* 10:1799–1810.

Zagotta, W. N., and R. W. Aldrich. 1990b. Voltage-dependent gating of *Shaker* A-type potassium channels in Drosophila muscle. *Journal of General Physiology.* 95:29–60.

Zagotta, W. N., T. Hoshi, and R. W. Aldrich. 1989. Gating of single *Shaker* potassium channels in *Drosophila* muscle and in *Xenopus* oocytes injected with *Shaker* mRNA. *Proceedings of the National Academy of Sciences, USA.* 86:7243–7247.

Zagotta, W. N., T. Hoshi, R. W. Aldrich. 1990. Restoration of inactivation in mutants of *Shaker* potassium channels by a peptide derived from ShB. *Science.* 250:568–571.

Zagotta, W. N., T. Hoshi, J. Dittman, and R. W. Aldrich. 1994. *Shaker* potassium channel gating II: transitions in the activation pathway. *Journal of General Physiology.* 103:279–319.

Zimmerberg, J., F. Bezanilla, and V. A. Parsegian. 1990. Solute inaccessible aqueous volume changes during opening of the potassium channel of the squid giant axon. *Biophysical Journal.* 57:1049–1064.